New constraints on the age and origin of the Dunbrack Pb-Cu-Zn-Ag deposit, Musquodoboit Batholith, southern Nova Scotia

Daniel J. Kontak[1], Kevin Ansdell[2], and Douglas Archibald[3]

[1]*Nova Scotia Department of Natural Resources, P.O. Box 698, Halifax, Nova Scotia B3J 2T9, Canada*
[2]*Department of Geological Sciences, University of Saskatchewan, Saskatoon, Saskatchewan S5W 0W0,*
Canada
[3]*Department of Geological Sciences, Queen's University, Kingston, Ontario K7L 3N6,*
Canada

Mineralization at the Dunbrack Pb-Zn-Cu-Ag deposit occurs within a ca. 1 m wide quartz vein characterized by comb, cockade, crustiform, and breccia textures. The mineralized vein, NW-trending and steeply dipping, has a medium- to coarse-grained, biotite-muscovite±cordierite monzogranite phase of the 370 Ma Musquodoboit batholith as its hanging wall and a fine-grained felsic dyke rock as its footwall. Silicate mineralogy in the vein is dominated by quartz with trace amounts of K-feldspar (Or_{86-100}), muscovite (≤ 2 wt. % FeO, ≤ 0.8 wt. % F), chlorite, and kaolinite, whereas sulphides include Fe-poor sphalerite (≤ 4 wt. % Fe), galena, chalcopyrite, and a variety of secondary Cu sulphides. Dating ($^{40}Ar/^{39}Ar$) of vein muscovite and the footwall dyke rock indicate similar ages of 370 Ma; therefore, vein formation and dyke injection are interpreted to be coincident with emplacement of the 370 Ma Musquodoboit Batholith.

Fluid inclusion studies of aqueous, L-V inclusions indicate homogenization temperatures of ca. $140 \pm 5°C$ and salinities of 20 ± 2 wt. % eq. NaCl, but minor amounts of inclusions with higher (24 to 27 wt. %) and lower (8-16 wt. %) salinities occur. First melting temperatures and analysis of decrepitate mounds indicate two fluid types, a more abundant $NaCl-H_2O$ fluid and a less abundant $NaCl-CaCl_2-KCl-H_2O$ fluid.

Sulphur isotopes for hypogene galena, chalcopyrite, and sphalerite are uniform and equate to $\delta^{34}S_{H_2S}$ of +4.2 to +6.6‰ (at 300°C), which is similar to data for other granite-related sulphide mineralization in the Meguma Zone. Vein quartz has an $\delta^{18}O$ value of $+15.3 \pm 1.2$‰ (n=10), which equates to $\delta^{18}O_{water}$ of +9 to +11.5‰ at 300°C, whereas fluid inclusion extracts indicate δD values of -90 to -113‰ (n=6).

Collectively, the timing of mineralization (i.e., 370 Ma) and the dominantly magmatic isotopic and geochemical signature for the vein-forming fluid suggest a genetic association with the Musquodoboit Batholith. However, the Ca-rich nature of some fluid inclusions and low δD values of fluid extracts suggest involvement of another reservoir, possibly reflecting a fluid that equilibrated with the country rock of the Meguma Group.

La minéralisation au dépôt de Pb-Zn-Cu-Ag Dunbrack se produit dans une veine de quartz d'une largeur c. 1 m caractérisée par des textures de peignes, cockade, croûteuses et de brèches. La veine minéralisée en direction nord-ouest a un pendage à pente forte, et une phase à grain grossier, de biotite-muscovite±cordierite monzogranite provenant du batholite Musquodoboit de 370 Ma en tant que lèvre supérieure et à un dyke a grain fin de roche felsique en tant que sa lèvre inférieure. La minéralogie de silicate dans la veine est dominée par le quartz avec des traces de K-feldspath (Or_{86-100}), muscovite (≤ 2 poids en pour-cent de FeO, ≤ 0.8 poids en pour-cent de F), chlorite, et kaolinite, tandis que les sulfures incluent la sphalérite pauvre en Fe (≤ 4 poids en pour-cent de Fe), la galène, la chalcopyrite, et une variété de sulfures secondaires de Cu. La datation ($^{40}Ar/^{39}Ar$) de la veine de muscovite et du dyke de roche a lèvre inférieure indiquent des âges semblables de 370 Ma ; donc, la formation de veine et l'injection de dyke sont interprétées pour être coïncidentes avec la mise en place Batholite Musquodoboit de 370 Ma.

Les études d'inclusions fluides « L-V » et aqueuses, indiquent les températures d'homogénéisation de c.$140 \pm 5°C$ et salinités de 20 % équivalent poids en pour-cent ± 2 NaCl, mais a des quantités mineures d'inclusions avec plus haut (24 à 27 poids %) et abaissement (8-16 poids %) des salinités produites. Les premières températures et analyse de fonte des monticules décrépités indiquent deux types de liquides, un fluide plus abondant de NaCl-HÒ et un fluide moins abondant de $NaCl-CaCl_2$-KCl-HÒ.

Les isotopes de soufre pour la galène hypogée, la chalcopyrite, et la sphalérite sont uniformes et égalisent à $\delta^{34}S_{H_2S}$ of +4.2 to +6.6l (à 300°C), semblable a des données pour d'autre minéralisation de sulfure jumeler au granite dans la zone de Meguma. Le quartz de veine a une valeur de $\delta^{18}O$ +15,3 ± 1.2l (n=10), qui égalise à $\delta^{18}O_{eau}$ de +9 à +11.5l à 300°C, tandis que les extraits liquides d'inclusion indiquent des valeurs de δD de -90 à -113l (n=6).

Collectivement, la synchronisation de la minéralisation (c.-à-d., 370 Ma) et la signature isotopique et géochimique principalement magmatique pour le fluide provenant de veine suggèrent une association génétique avec le Batholite de Musquodoboit. Cependant, la nature riche en calcium de quelques inclusions liquides et valeurs basses δD d'extraits liquides suggèrent la participation d'un autre réservoir, reflétant probablement un fluide qui a équilibré avec la roche de la région du Groupe de Meguma.

[Traduit par la rédaction]

INTRODUCTION

The Dunbrack Pb-Cu-Zn-Ag deposit, located 4.8 km northwest of the village of Musquodoboit Harbour east of Halifax, represents vein-type mineralization within the 370 Ma Musquodoboit Batholith (Fig. 1). The deposit was discovered in 1888 and worked intermittently over the next 40-50 years via two shafts sunk in order to evaluate the extent of the mineralization (i.e., several 100 t of a few % Pb and minor Cu and Ag). The deposit is unusual because of (1) the association of tridymite - pyromorphite - meneghinite (Friedlaender 1968, 1970; Chatterjee 1977) and other minerals (see below), which are unique to this part of the Musquodoboit Batholith and mineralized granites within the Meguma Zone, (2) vein textures (e.g., comb, cockade) reminiscent of epithermal veins, and (3) a ^{40}Ar/^{39}Ar date on hydrothermal sericite(?) indicating an apparent age of ca. 304 Ma for mineralization and associated alteration (MacMichael 1975), which contrasts with the 370 Ma age for the host granite. Previous work on the deposit focused on vein mineralogy, textures, and fluid inclusions (MacMichael 1975; Dickie 1978). The present study was initiated because of the apparent similarity in time of formation between Dunbrack and the nearby, carbonate-hosted Gays River Zn-Pb deposit (Fig. 1) and the presence of similar mineralization elsewhere in the Meguma Zone, such as Tobeatic Lake (Corey 1995; Corey and Graves 1996) and Tangier Grand Lake (Corey 1993) (Fig. 1). In this paper we summarize the paragenesis and mineralogy of the vein, mineral and whole-rock geochemistry, fluid inclusion studies, stable isotope systematics, and ^{40}Ar/^{39}Ar geochronology.

GEOLOGICAL SETTING

The Dunbrack deposit is located in the central part of the 370 Ma Musquodoboit Batholith, the second largest intrusion in the Meguma Zone (Fig. 1). The batholith intruded metasedimentary rocks of the Lower Paleozoic Meguma Group. A narrow contact metamorphic aureole containing cordierite porphyroblasts is developed within a few hundred metres of the contact (Horne *et al.* 1998). The central part of the batholith is characterized by the presence of coarse cordierite grains in a two-mica leucomonzogranite host (MacDonald and Clarke 1985; Ham 1993), whereas the flanking parts of the batholith contain lesser amounts of cordierite. In the vicinity of the Dunbrack deposit (i.e., within 1 km) there occurs a fine-grained and texturally variable leucogranite, one of several that occur throughout the batholith. Fine-grained felsic dykes and pegmatites, with variable trends including NW (Ham 1998) are also present, one of which occurs adjacent to the mineralized vein (see below) (Fig. 2). Airborne radiometric surveys indicate that local areas of the batholith are underlain by fine-grained and/or texturally variable phases with high eU/eTh ratios (Ford 1993; Ham 1993; Fig. 1).

Numerous NW-trending faults cut the batholith (Jones and MacMichael 1976; MacDonald and Clarke 1985; Ham 1993, 1994). However, faults strongly influence the shape of the Musquodoboit Batholith and the adjacent South Mountain

Batholith (Horne *et al.* 1992), and thus were probably active at the time of batholith emplacement. The veins at Dunbrack may be related to left-lateral offset along a fault transecting Tangier Grand Lake (Jones and MacMichael 1976).
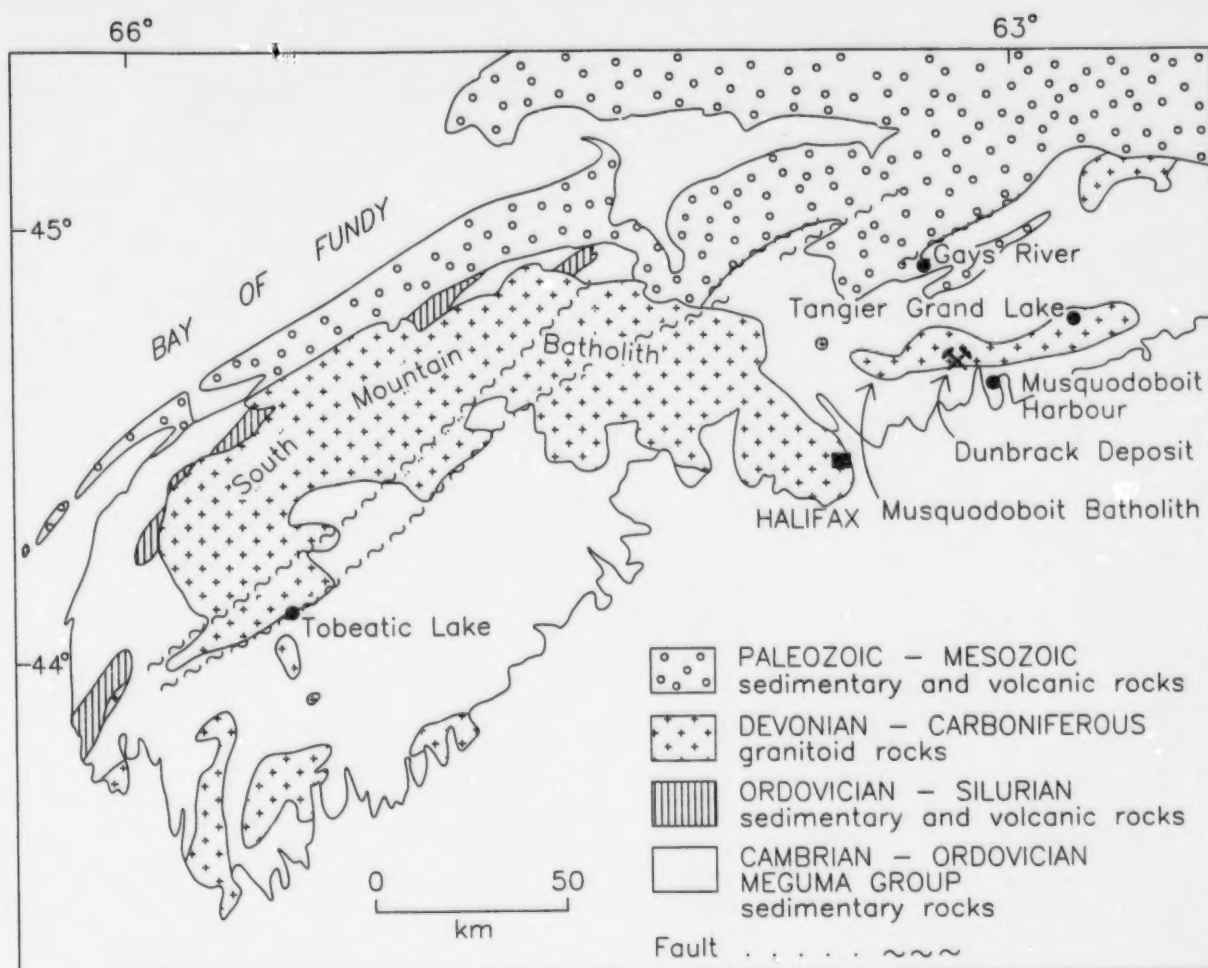
GEOLOGY OF THE DUNBRACK DEPOSIT

The following description of the Dunbrack deposit was extracted from summaries in assessment reports in Nova Scotia Department of Natural Resources files, theses of MacMichael (1975) and Dickie (1978), and observations by the senior author based on examination of material in dump piles. The mineralization occurs within a ≤ 1 m wide quartz-rich vein which pinches out vertically (inset Fig. 2), has a coarse leucomonzogranite hanging wall (HW) and fine grained, 1.2 m-wide dyke as a foot wall (FW) (Fig. 2). The vein, oriented 110° and dipping 62°N, was traced on surface for a distance of several 100 m and the ore grade decreases across the vein towards the HW. The dyke at the FW contact with the vein is very fine grained, highly altered, and reddish coloured as a result of hematite stain. The contact of the vein with the HW granite is a zone of silicification 1 to 3 cm wide. Based on the presence of chloritic and sericitic alteration of biotite and feldspar, respectively, in the granite, MacMichael (1975) contoured areas of increasing alteration, which showed a strong correlation with proximity to the mineralized vein (Fig. 2). This alteration suggests that the vein-forming fluids infiltrated outwards from the vein. The dyke rock is intensely altered to chlorite, hematite and sericite adjacent to the vein.

The character of the vein can be ascertained from the debris in the dump pile. Numerous boulders of brecciated material (Fig. 3) contain (1) angular fragments of altered dyke rock (red, hematitic, fine-grained, felsic rock), either in isolation or forming the nucleus of comb quartz overgrowths (i.e., cockade texture); (2) multiple layers of variably textured quartz, and (3) coarse galena occurring as massive clumps, as coarse to fine aggregates within a quartz matrix, or within altered fragments with other sulphides (e.g., chalcopyrite, sphalerite). Several generations of vein formation occurred with repeated brecciation of earlier material. Well-developed comb quartz, cockade and crustiform layers are all indicative of open-space infilling and epizonal conditions (e.g., Stanton 1972; Vearncombe 1993; Dong *et al.* 1995; Dong and Zhou 1996), but Dowling and Morrison (1988) noted that such textures may also occur in plutonic environments beneath epithermal settings.

MINERALOGY AND TEXTURES OF VEIN SAMPLES

The vein at Dunbrack consists of the following minerals: quartz, including tridymite(?), calcite, fluorite, galena, chalcopyrite, chalcocite, sphalerite, bornite, malachite, azurite, pyromorphite $[Pb(PO_4)_3Cl]$, meneghinite $(Pb_{13}CuSb_7S_{24})$, pyrrhotite, cerussite, ilmenite, djurleite $(Cu_{1.96}S)$, and digenite (Cu_9S_5). Assays of the vein indicate the presence of anomalous Au (to 30 ppm) and Ag (10's of ppm), but their mineralogic expression has not yet been determined. Details of the mineralogy are described below.
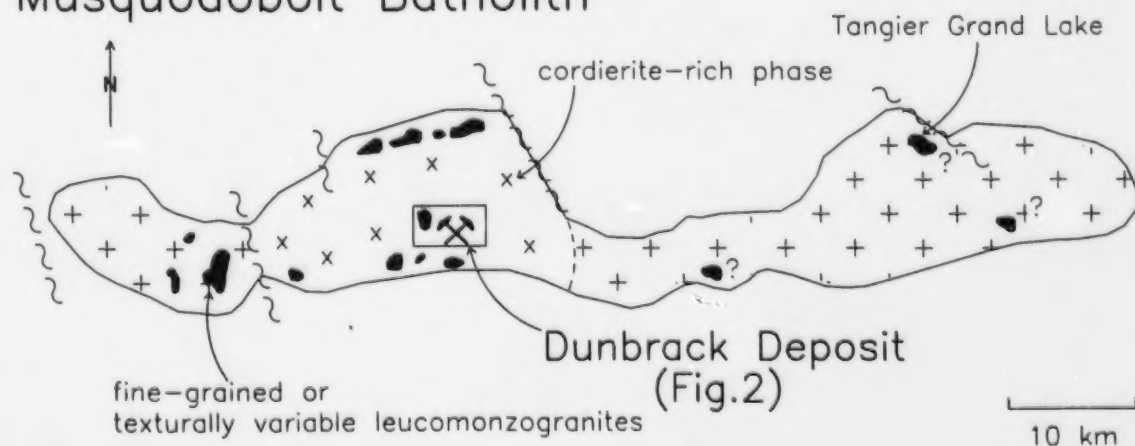
Fig. 1. Geological map of southern Nova Scotia showing the Musquodoboit Batholith (MB) and the location of the Dunbrack showing and other places mentioned in the text. Bottom diagram shows the general geology of the Musquodoboit Batholith (after Ham 1993, 1994, pers. commun., 1996).
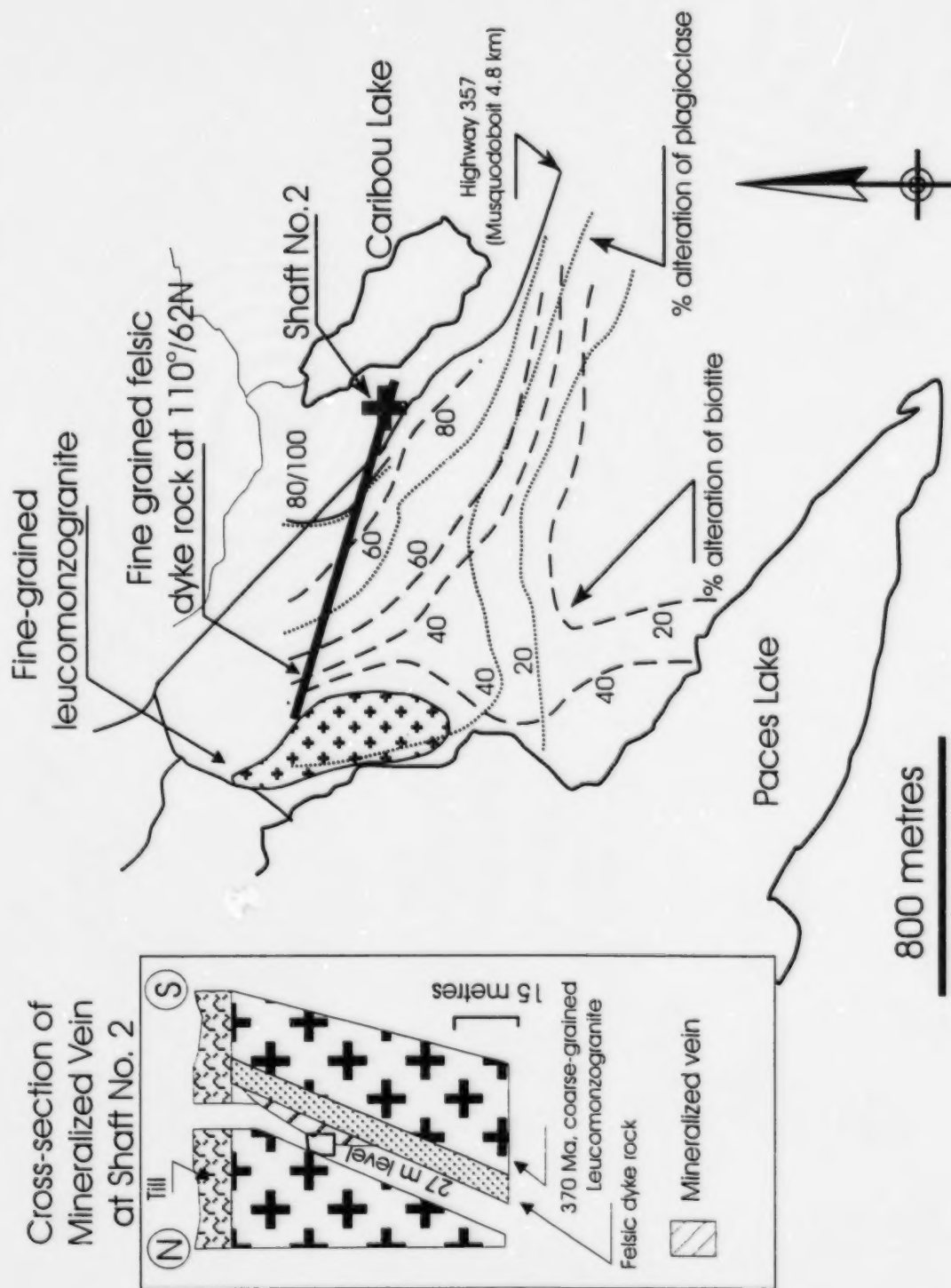
Fig. 2. Location of the Dunbrack deposit with contours for percentage of alteration of biotite to chlorite and feldspar to sericite in the Musquodoboit Batholith (after MacMichael 1975). The inset diagram of the deposit area shows a north-south cross-section (modified from Dickie 1978).
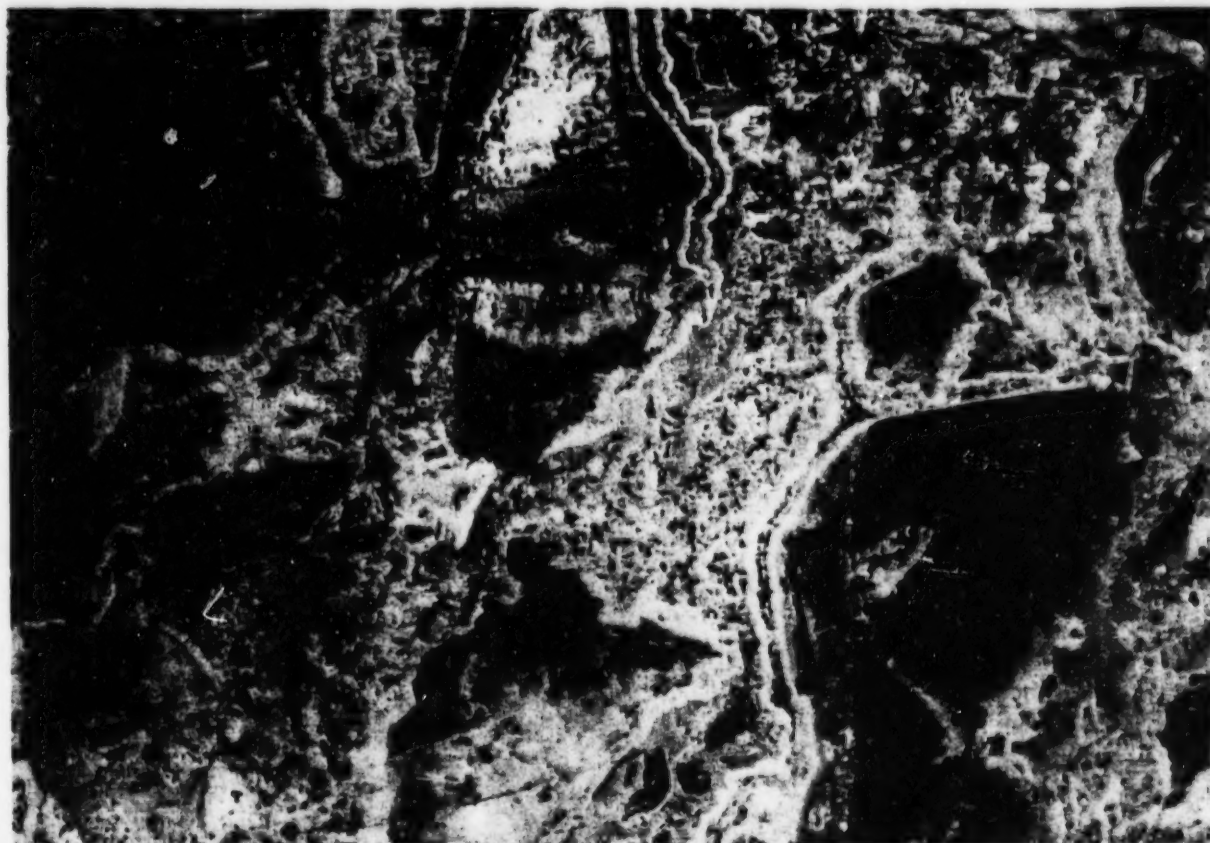
Fig. 3. Slab of vein breccia from the Dunbrack deposit illustrating the brecciated nature of the vein fill along with the cockade, crustiform, and comb textures. Note the very fine-grained, flour-textured material that is locally banded and the smoky colour of the quartz. Width of photo is 10 cm.

Vein Silicates

Silicate mineralogy, in descending order of abundance, includes quartz, K-feldspar (Kf), muscovite and chlorite (Fig. 4). Quartz occurs in several different habits, the most common being (1) flamboyant, (2) radially arranged acicular prisms in comb texture, with growth banding defined by numerous milky white zones containing abundant fluid and silicate inclusions, and (3) equant crystals in places occurring with Kf (Fig. 5). Trace amounts of muscovite occur in areas of quartz inundated with inclusions, whereas hematite is sporadically distributed throughout. Banding is defined by equant quartz succeeded by acicular flamboyant comb quartz which widens outwards from the base. Multiple layers or generations of quartz may occur within a single sample. In areas of brecciation, angular pieces of quartz suggest fragmentation or comminution of massive quartz vein material. K-feldspar occurs as equant to anhedral grains intergrown with quartz and may account for 30 to 40% of some areas of the vein (Fig. 5); it is commonly altered to hematite or kaolinite. In some glomeroclasts (see below) granophyric textures occur. Muscovite occurs as coarse, equant to tabular grains that may be bent or kinked (Fig. 5), within the quartz vein or as part of altered fragments coexisting with quartz and Kf. Muscovite
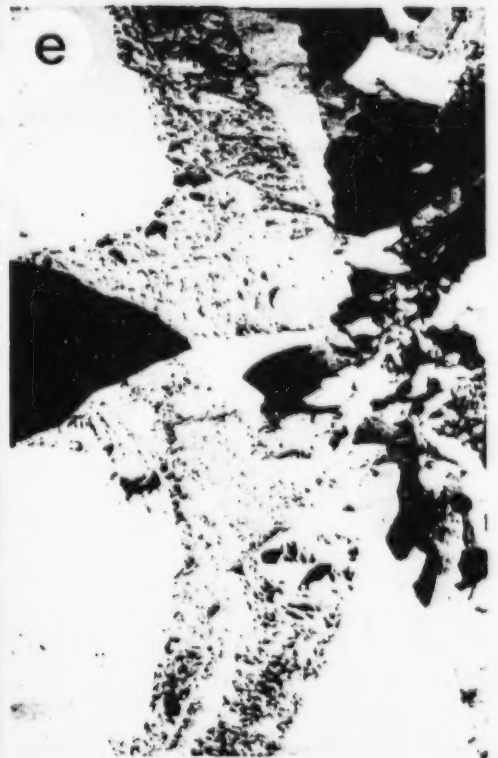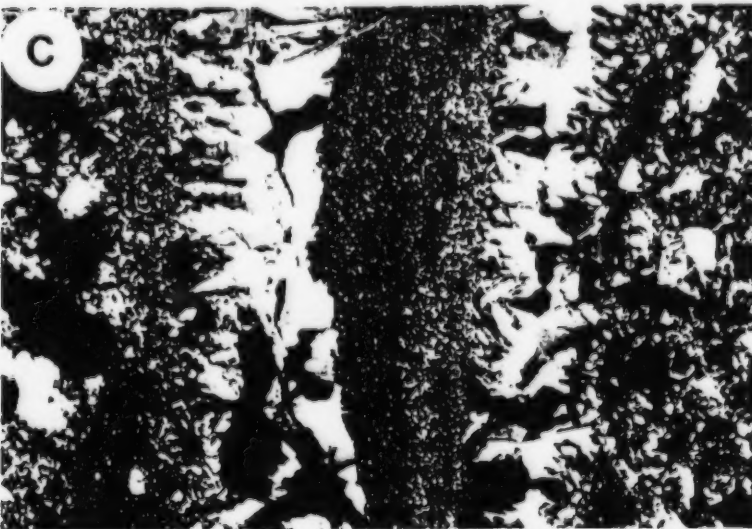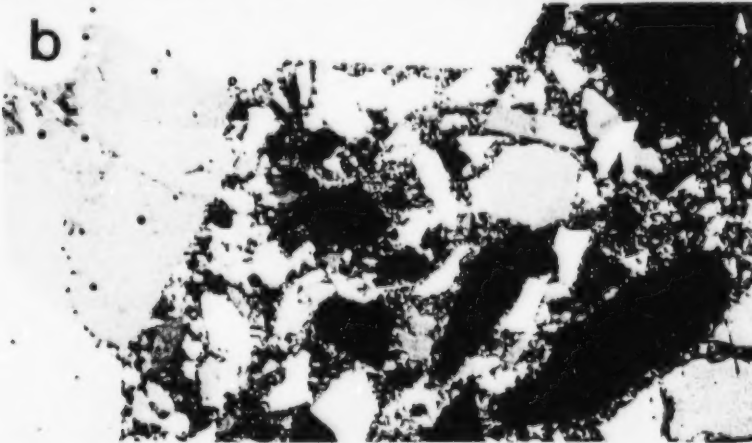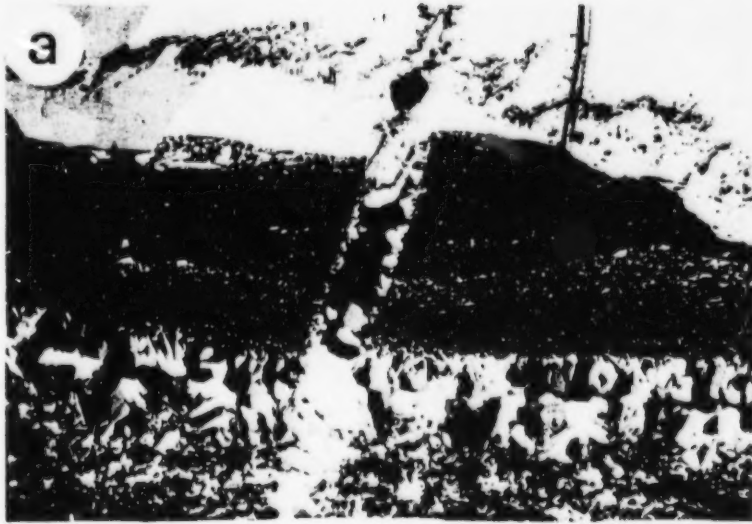
may be partially replaced by quartz and also occurs as small grains disseminated in cores of quartz grains. Chlorite is rare and probably represents altered biotite. Fragments of altered granite(?) also occur in the vein (Fig. 5).

Also present in the vein are oval, equant, and irregularly-shaped areas of coarser-grained (i.e., relative to the matrix material of the vein), equigranular, glomeroclastic aggregates of quartz, Kf, muscovite, chlorite/biotite, in which hematite and kaolinite, after Kf, are common (Fig. 5). The quartz in this occurrence may contain small euhedral zircon.

The matrix to the coarse vein material consists of very fine-grained (i.e., grain size of a few μm) material with a banded texture that is perpendicular to the comb quartz fabric (Fig. 4b, c, d, e). This material is reddish in hand specimen as a result of hematitic alteration, perhaps after feldspar. Fragments of this material are common in the vein.

Ore Mineralogy of the Vein

The ore mineralogy is dominated by hypogene galena, chalcopyrite and sphalerite with lesser amounts of supergene Cu sulphides (Fig. 6). The primary sulphides occur infilling original porosity where quartz terminates as euhedral crystals in open spaces, or as disseminations in the matrix of fine-

grained vein material. The supergene minerals rim chalcopyrite or form along fractures with the alteration widest at grain margins and tapering inwards. The assemblage of secondary minerals is variable and several minerals may be intergrown with complex textural relationships.

ANALYTICAL TECHNIQUES

Major and trace element compositions were obtained on a sample of dyke rock using wet chemical techniques at DalTech, formerly TUNS, in Halifax, and also at Memorial University of Newfoundland using solution ICP-MS (Jenner *et al.* 1990). Mineral chemistry was done at Dalhousie University using a JEOL Superprobe (details in Kontak and Smith 1993). Details of stable isotope data (at the University of Saskatchewan) and fluid inclusion studies (at the Nova Scotia Department of Natural Resources) are fully described in Kontak *et al.* (1996) and Kontak (1998), respectively. The procedures for $^{40}Ar/^{39}Ar$ dating (at Queen's University) are given in Erdmer *et al.* (1998).

$^{40}Ar/^{39}Ar$ Dating

A sample of altered, fine-grained, reddish felsic dyke rock occurring as fragments in vein breccia and a hand-picked separate of coarse-grained muscovite from a silicate-sulphide vein sample were dated using the $^{40}Ar/^{39}Ar$ method. The age spectrum for the whole-rock sample (Fig. 7a; Table 1) is characterized by ages of ca. 360 to 370 Ma for the first 35% of the gas, but with large errors related to the low potassium content and "dirty" nature of the sample. The central part of the age spectrum has ages of 330 to 355 Ma and the high temperature steps have ages of ca. 280 Ma. The integrated age for this sample is 335 ± 17 Ma and the isotope correlation age is 354 ± 56 Ma.

The age spectrum for the muscovite separate (Fig. 7b; Table 1) is characterized by a hump for the low temperature steps which give ages of ca. 385 Ma, but the majority (94%) of the release spectrum consists of steps that fall in the narrow interval of 369 to 376 Ma. The highest temperature analyses (54% of total gas) define a plateau age of 368.5 ± 3.0 Ma. The integrated age for the sample is 370.5 ± 2.5 Ma.

Seventeen spot dates on muscovite (Table 1) from the mineral separate indicate apparent ages of 366 to 373 Ma, except for one anomalous age of 404 Ma, and integrated and correlation ages identical to the age spectrum (Fig. 7b).

Fig. 5. Back-scattered electron image of vein material illustrating a hypidiomorphic texture for material consisting of quartz (Qtz), K-feldspar (Kf), and muscovite (Ms). Other abbreviations: fragment (Frg).

Fig. 4. Photomicrographs (all cross nicols) of vein samples from the Dunbrack deposit. (a) Vein sample illustrating series of events which start with crystallization of fine-grained matrix material (stage 1), growth of comb quartz layers after vein opening to generate open space (stage 2), and finally a cross vein (stage 3) which cross cuts all the above. Width of photo is 1.2 cm. (b) Brecciated quartz fragments and fine-grained matrix material infilling space lined with coarse quartz euhedra. Note the bimodal grain size for vein fill, lack of undulose extinction in the quartz, and absence of any comb or flamboyant textures in the quartz fragments. Width of photo is 2.0 cm. (c) Vein sample with textures indicating multiple stages of vein growth both in the left and right of photo. Note that the quartz in the centre layer is truncated by an unconformity surface. Width of photo is 2.0 cm. (d) Detail of part of the sample shown in Fig. 4c to illustrate the banding in the matrix material (flowage feature?) and the comb quartz layers, the textures of which indicate infilling of open space as in a vein with the matrix material at top and bottom forming the substrate. Width of photo is 1 cm. (e) Comb quartz in detail showing the presence of primary growth faces as outlined by areas inundated by fluid inclusions. The dark areas in the growth bands are void spaces. Width of is photo 1.6 mm.
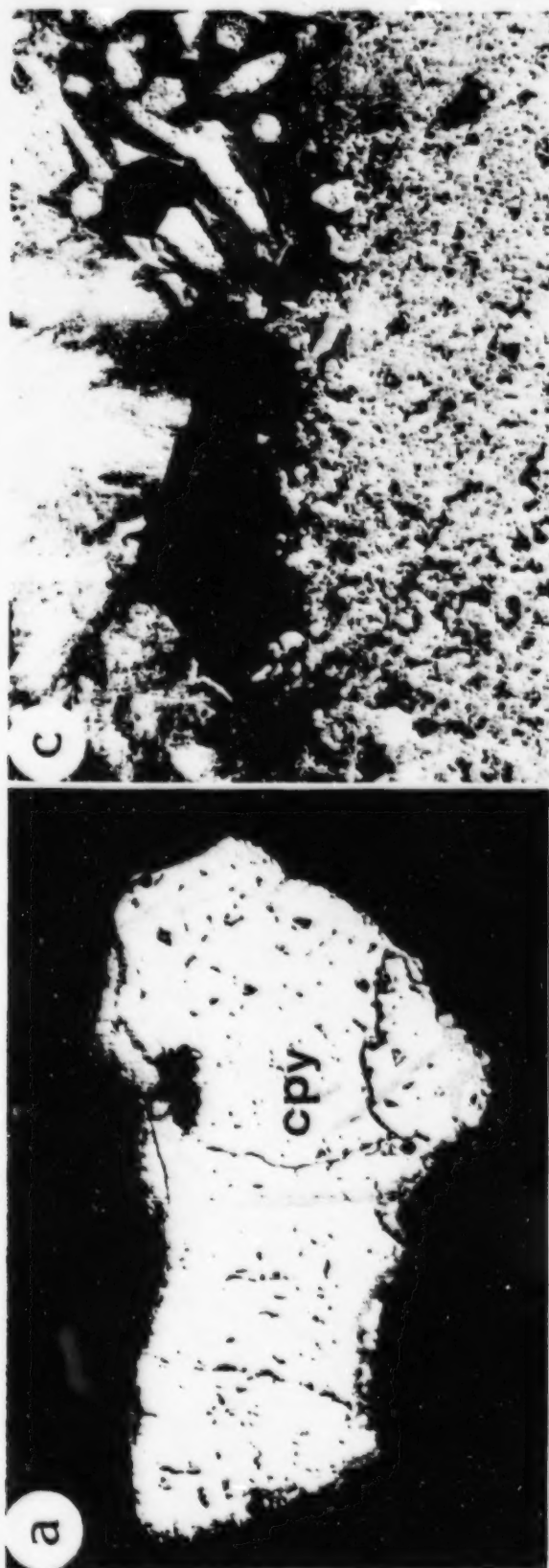
Fig. 6. Reflected light (a, b) and transmitted light (c) photomicrographs of ore minerals at Dunbrack. (a, b) Chalcopyrite (cpy) filling open space between euhedral quartz grains. The chalcopyrite is cut and rimmed by secondary Cu-Fe sulphides (cc), including covellite, bornite, djurleite and chalcocite, and surrounded by galena (gal). Widths of photos in a and b are 1.2 mm and 0.3 mm, respectively. (c) Sphalerite (centre of photo) between comb quartz (top) and fine-grained matrix material containing disseminated galena (black). Width of photo is 1.2 mm.

Table 1. Summary of data for ^{40}Ar/^{39}Ar step-heating and laser dating of Dunbrack samples.

|	^{36}Ar/^{40}Ar (X 0.00001)	^{39}Ar/^{40}Ar (X 0.001)	Ca/K	%^{40}Ar (atm)	%^{39}Ar	^{40}Ar*/^{39}Ar	Age (±) Ma
DB-96-3 Muscovite; Laser Step Heating; J Value = 0.007529							
Step							
1	110.66(85.5)	44.64(2.30)	0.00	32.63	0.38	15.080(1.289)	194.01(15.72)
2	64.02(26.2)	29.55(0.70)	0.00	18.90	1.04	27.430(0.589)	338.70(6.64)
3	18.88(16.7)	29.88(0.50)	0.03	5.57	1.55	31.595(0.393)	384.99(4.32)
4	4.34(10.1)	30.99(0.42)	0.40	1.28	3.30	31.846(0.384)	387.74(4.20)
5	3.73(8.00)	32.04(0.35)	1.39	1.10	5.74	30.861(0.300)	376.92(3.31)
6	3.92(8.20)	32.18(0.34)	1.69	1.16	8.23	30.715(0.285)	375.31(3.14)
7	4.4(9.60)	32.28(0.42)	1.83	1.30	9.27	30.567(0.343)	373.67(3.79)
8	6.19(10.0)	32.24(0.36)	2.92	1.83	8.74	30.441(0.280)	372.29(3.10)
9	7.65(10.6)	32.23(0.40)	3.48	2.26	7.56	30.317(0.314)	370.91(3.47)
10	8.26(10.2)	32.43(0.38)	3.15	2.44	7.33	30.076(0.304)	368.24(3.36)
11	8.81(10.0)	32.48(0.40)	3.27	2.60	14.00	29.984(0.315)	367.23(3.49)
12	9.55(11.2)	32.44(0.43)	3.04	2.82	5.37	29.955(0.338)	366.90(3.75)
13	10.03(11.1)	32.14(0.41)	3.36	2.96	27.51	30.185(0.325)	369.46(3.60)
DB-96-3 Muscovite; Laser Spot Dates; J Value = 0.007412							
Spot							
1	0.004(154.6)	29.48(2.75)	0.01	0.01	0.10	33.81(15.99)	404.51(170.89)
2	46.03(5.75)	28.14(0.46)	0.01	13.59	2.71	30.69(0.79)	369.83(8.61)
3	12.56(8.02)	32.12(0.57)	0.01	3.71	1.63	29.97(0.91)	361.92(10.02)
4	9.23(8.15)	32.08(0.60)	0.01	2.73	1.74	30.31(0.85)	365.69(9.33)
5	2.90(2.76)	32.15(0.46)	0.01	0.86	5.89	30.83(0.49)	371.33(5.39)
6	4.69(3.85)	32.17(0.45)	0.01	1.39	3.11	30.65(0.56)	369.36(6.12)
7	5.79(6.43)	32.11(0.63)	0.01	1.71	1.86	30.60(0.84)	368.81(9.22)
8	15.52(5.06)	31.88(0.52)	0.01	4.58	3.19	29.92(0.62)	361.36(6.84)
9	5.80(1.51)	31.83(0.29)	0.01	1.71	13.14	30.87(0.30)	371.77(3.31)
10	5.57(2.79)	32.39(0.41)	0.01	1.64	4.71	30.35(0.46)	366.14(5.07)
11	11.46(1.47)	31.42(0.28)	0.01	3.38	9.77	30.74(0.31)	370.32(3.39)
12	50.01(2.76)	27.67(0.31)	0.01	14.77	7.61	30.79(0.45)	370.86(4.96)
13	5.25(7.77)	31.85(0.58)	0.01	1.55	1.49	30.90(0.92)	372.10(10.05)
14	3.52(10.54)	32.09(0.86)	0.01	1.04	1.20	30.83(1.29)	371.34(14.03)
15	3.49(0.81)	32.14(0.30)	0.01	1.03	22.45	30.79(0.30)	370.87(3.29)
16	2.45(3.07)	32.03(0.38)	0.01	0.73	5.50	30.98(0.43)	272.98(4.69)
17	1.36(2.71)	32.16(0.29)	0.01	0.40	13.90	30.96(0.29)	372.76(3.21)
DB-96-5 Whole Rock; Step-Wise Heating; J Value = 0.007277							
Step							
1	330.98(30.56)	0.68(0.36)	0.05	97.79	0.21	32.41(126.07)	382.07(133.39)
2	318.49(22.70)	1.93(0.43)	0.05	94.09	1.37	30.53(24.75)	361.98(265.89)
3	308.82(9.17)	2.24(0.11)	0.05	91.24	9.87	38.97(11.33)	450.46(115.92)
4	249.64(13.47)	8.26(0.32)	0.05	74.74	8.09	31.74(4.69)	374.91(50.09)
5	109.05(21.44)	22.15(0.72)	0.05	32.19	6.75	30.59(2.94)	362.61(31.66)
6	135.22(20.64)	19.24(0.64)	0.05	39.93	10.28	31.20(2.32)	369.14(24.92)
7	115.89(26.76)	21.96(1.01)	0.05	34.21	5.65	29.94(3.83)	355.68(41.31)
8	74.90(52.49)	27.25(2.83)	0.05	22.10	8.69	28.57(5.59)	340.81(60.8)
9	66.28(35.65)	2.87(1.26)	0.05	19.55	5.76	27.98(3.28)	334.4(35.78)
10	75.56(32.78)	28.24(1.16)	0.05	22.28	7.35	27.50(2.93)	329.16(32.07)
11	123.31(32.87)	27.10(1.03)	0.05	36.35	6.26	23.47(3.37)	284.52(37.79)
12	237.76(16.13)	13.35(0.48)	0.05	70.13	29.72	22.33(1.85)	271.73(20.96)
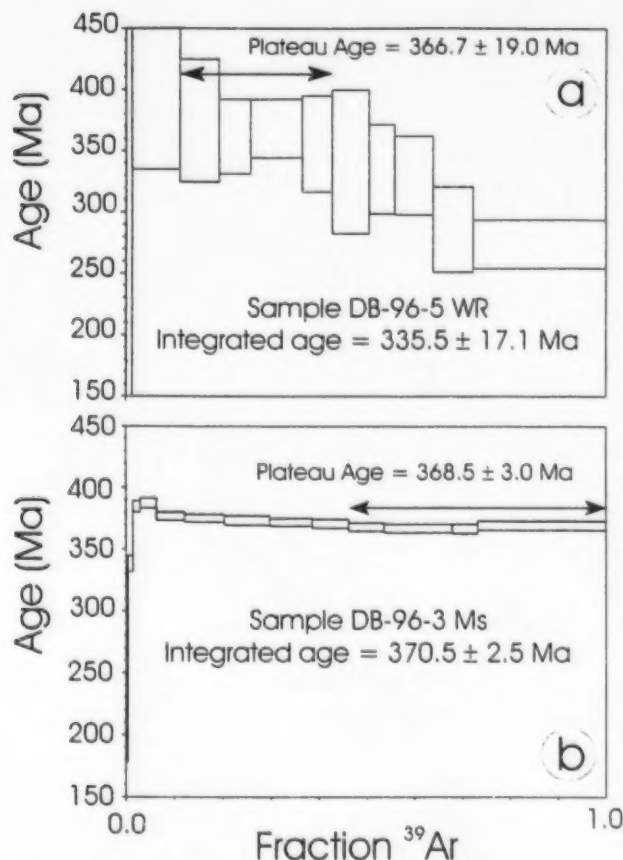
Fig. 7. ^{40}Ar/^{39}Ar age spectrum plots for samples of fine-grained felsic dyke rock forming footwall to vein (DB-96-5 WR) and vein muscovite (DB-96-3 Ms) from Dunbrack.

WHOLE-ROCK AND MINERAL CHEMISTRY

Dyke Rock

A single sample (DB-96-5) of the fine-grained, reddish material used for dating purposes, possibly representing altered dyke rock that forms the hanging wall to the mineralized vein, was analysed. The analysis indicates 97.8 wt. % SiO_2, 2.5 wt. % Al_2O_3 and minor to trace Na_2O (0.14), CaO (0.35), K_2O (0.2), MgO (0.87), P_2O_5 (0.08), MnO (0.013) and TiO_2 (0.013). Thus, the data indicate that the dyke rock has been intensely silicified, at least locally. Rastering analysis of similar material using the electron microprobe (at Dalhousie University) also indicates that the material is highly altered, with a composition dominated by silica and alumina, but with up to 3-4 wt. % FeO and 1-2 wt. % K_2O locally.

Trace element analyses indicate the following (in ppm): Rb=42, Li=18, Sr=42, Mo<1, Cs=3, Ba<1, Pb=300, U=3.7, Th=1.2, Zr=12. Of note with respect to the trace element chemistry is that the U/Th ratio of 2.5 is similar to that of felsic rocks in general, and that the Zr content is high for a hydrothermal sample, possibly suggesting the presence of relict zircon. A chondrite-normalized plot for rare earth element (REE) data (Fig. 8) indicates a surprising enrichment in REE, in particular the LREE, given the high silica content of the sample. The REE profile is LREE enriched, strongly fractionated (La_N/Lu_N = 250), and has a negative Eu anomaly (Eu_N/Eu_N^* = 0.23). In contrast, dyke rocks and porphyries from the Musquodoboit Batholith (after MacDonald and Clarke 1985) are relatively depleted in REE and less fractionated (Fig. 8).

Vein Minerals

Alkali feldspar is homogeneous with no exsolution lamellae of albite observed, has compositions ranging between $Or_{86}Ab_{14}$ and Or_{100} (Fig. 9a; Table 2), and may contain up to 0.4 wt. % P_2O_5. Muscovite is phengitic with up to 2 wt. % FeO and minor MgO (Table 2), and contains a maximum of 0.8 wt. % F with an inverse correlation between F and FeO (i.e., the Fe-F avoidance principle; Fig. 9b). Data for muscovite from the Musquodoboit Batholith indicate only trace amounts of F (L. Ham, personal communication, 1998). Chlorine was not detected in any of the muscovite grains analysed. Chlorite, after biotite, is ripidolitic in composition with Fe/(Fe+Mg) values of 0.6 to 0.7 (Table 2). Kaolinite was also analysed and stoichiometric chemistry obtained (Table 2).

Analyses of sulphides (Table 3) indicate that galena is generally pure with only trace amounts of Ag detected in a few analyses. Sphalerite is Fe-poor with a maximum of 4 wt. % Fe, but most analyses show Fe to be below the detection limit (i.e., <0.2 wt. % Fe). Grains may be optically zoned and the highest Fe is found in reddish as compared to yellow-red areas. Chalcopyrite and bornite are stoichiometric with no impurities. Secondary sulphides analysed include a variety of Cu sulphides (i.e., covellite (CuS), $Cu_{11}S_9$, $Cu_{11}S_9$, Cu_3FeS_4, Cu_5FeS_4) and variable mixtures of Cu-Fe-Pb-S, Cu-Pb-S, Zn-Cu-Fe-S. In the case of the latter phases (i.e., mixtures), some contamination from underlying phases is a possibility and further work will be required to clarify this mineralogy. The highest concentration of Ag (to 2.5 wt. %) is found in an unidentified Cu-Pb-S mineral (Table 3).

FLUID INCLUSION STUDIES

Petrography

Representative samples of vein quartz were cut to 150 μm and doubly polished for fluid inclusion petrography. The samples are similar, with three inclusion types dominant and a rare fourth type (Fig. 10a). The most abundant inclusions are irregular-shaped to equant aqueous inclusions of ≤5 to 30 μm with highly variable liquid:vapor (L:V) ratios; in fact, the dominance of monophase L- and V-rich types suggest post-entrapment modification (i.e., necking). The irregular-shaped inclusions are far more abundant (i.e., >90%) than the equant inclusions. This population of inclusions (Fig. 11a, b, c) occurs along growth zones in quartz (i.e., primary origin) and along healed fracture planes (i.e., secondary or pseudosecondary origin). The second type of inclusions are equant to elongate, two-phase L-V inclusions mostly ≤20-30 μm, but up to 150 μm, that occur along healed fracture planes in clear quartz or rarely cross-cutting milky white quartz (Figs. 10b, 11d, e, f, g). These inclusions are conservatively
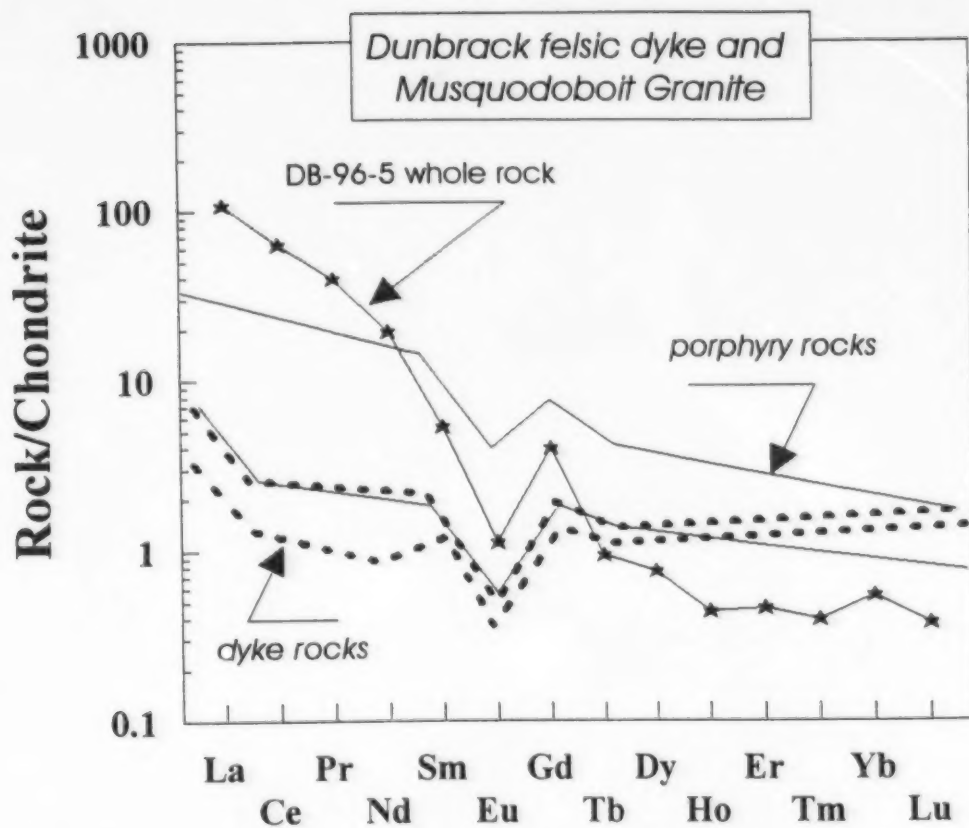
Fig. 8. Chondrite-normalized rare-earth element plot for sample of the fine-grained, reddish material (altered dyke rock?) from Dunbrack, together with data for porphyry and dyke rocks in the Musquodoboit Batholith (MacDonald and Clarke 1985). Note the enrichment of light rare-earth elements and strongly fractionated pattern for DB-96-5 compared to the other rocks.

classified as secondary, although some may in fact be pseudosecondary. The third type of inclusions includes equant to irregular-shaped monophase, L-type inclusions, ca. 10-20 μm in length, occurring along healed fracture planes (Fig. 11h). The fourth inclusion type, confined to a single locality in one sample (Fig. 10c), consists of liquid petroleum and its composition was confirmed by its fluorescence under UV light.

Thermometric measurements

Homogenization measurements (T_h) were determined for four quartz samples containing type 2 inclusions, some of which occur with type 4 inclusions, and very uniform results were obtained, as summarized in Figure 12. The range of T_h measurements for all inclusions was 124° to 151°C, but 95% of the data fall in the range of 134° to 142°C and in any group of inclusions the range is ≤ 1°C (e.g., area in Figure 11e). These results contrast to the data of Dickie (1978; Fig. 12a) in which a much larger range of T_h was obtained. The reason for the discrepancy between the two studies is unclear, although one possibility is that necked inclusions may have been included in the population studied by Dickie (1978), as a similarly large range in T_h was observed for groups of inclusions with variable L:V ratios (i.e., necked inclusions),

although such data are not presented in Figure 12a.

Freezing of inclusions indicated that first melting occurred at either -50° to -40°C or -28° to -21°C, which indicates that fluids contained additional cationic species in solution other than NaCl in the former group, probably Ca and Mg (Roedder 1984; Crawford 1981). Melting of hydrohalite occurred at three different intervals: -35° to -30°C, -23° to -21°C and rarely (n=4) -15° to -5°C; thus, variable $NaCl/(NaCl+CaCl_2)$ ratios are indicated. However, ca. 90% of inclusions have hydrohalite melting near -21°C, thus the fluids are best approximated by the $NaCl-H_2O$ system with minor amounts of a $NaCl-CalCl_2-H_2O$ fluid. Last melting of ice and hydrohalite indicates that inclusion salinity (Fig. 12b) is 20 ± 2 wt. % eq. NaCl, with a few inclusions exhibiting both higher (i.e., 24 to 27 wt. %) and lower (i.e., 8 and 16 wt. %) salinities. Thus, at least two distinct fluid compositions are indicated by the freezing experiments, a dominant $NaCl-H_2O$ fluid of ca. 20 wt. % eq. NaCl, and a second, much less abundant (i.e., <5% of inclusions), of $NaCl-CaCl_2-H_2O$ composition but with similar salinity.

It is also noted that type 2 inclusions occurring with type 1 and 3 inclusions have salinities of ca. 20 wt. % NaCl, which suggests that similar fluids are represented by these inclusion populations.

Table 2. Representative analyses of vein silicates, Dunbrack deposit, Nova Scotia.

Sample Point	K-feldspar DB-96-8 6	DB-96-8 7	DB-96-8 8	DB-96-8 12	Chlorite DB-96-8 1	DB-96-8 2	Kaolinite DB-96-10 3
SiO_2	63.61	63.30	63.85	64.14	31.28	29.40	47.06
Al_2O_3	18.57	18.71	18.65	18.78	17.82	16.64	33.81
FeO	*	*	*	*	21.81	26.73	1.77
MnO	*	*	*	*	0.24	0.22	*
MgO	*	*	*	*	6.14	5.59	0.25
CaO	nd	nd	nd	nd	0.20	0.15	*
Na_2O	1.06	0.90	0.95	1.08	1.83	1.78	0.23
K_2O	14.92	15.62	15.19	15.22	0.79	0.71	0.17
P_2O_5	nd	nd	0.35	0.40	*	*	*
Total	98.16	98.53	98.99	99.62	80.11	81.22	83.29

| Sample Point	Muscovite DB-96-8 9	DB-96-8 10	DB-96-5 6	DB-96-5 12	DB-96-5 13	DB-96-5 16	DB-96-3 1	DB-96-3 3
SiO_2	46.05	45.97	46.50	46.33	45.48	44.79	46.91	47.57
TiO_2	0.82	0.76	0.44	nd	0.31	0.63	nd	nd
Al_2O_3	34.67	35.02	35.67	34.91	34.69	34.50	34.27	35.41
FeO	1.34	1.42	1.18	1.49	1.41	1.24	2.09	1.79
MnO	nd	nd	nd	nd	nd	nd	nd	nd
MgO	0.71	0.74	0.74	1.06	0.83	0.92	1.31	1.01
CaO	nd	nd	nd	nd	0.72	nd	nd	nd
Na_2O	0.49	0.54	0.52	0.67	0.72	0.78	0.45	0.42
K_2O	8.40	8.70	8.73	9.74	9.65	9.82	9.76	9.92
F	0.31	0.29	nd	0.43	0.45	0.80	0.64	0.38
Cl	nd	nd	nd	nd	nd	nd	nd	nd
Total	84.39	93.44	93.78	94.63	94.26	93.48	95.43	96.50

Note: *, element not analyzed; nd, below detection limits (0.2%)
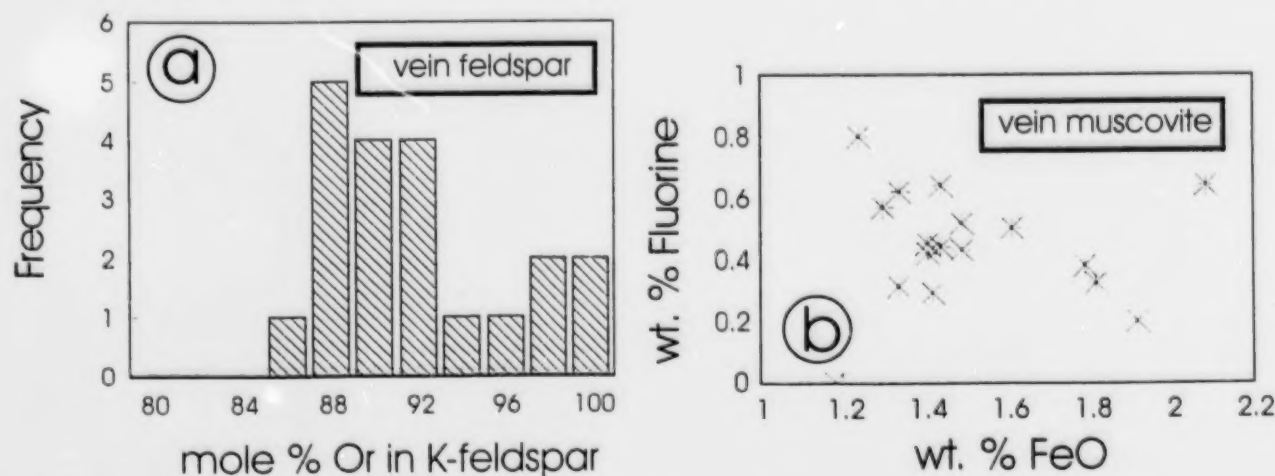
Fig. 9. Mineral chemistry for Dunbrack samples. (a) Histogram plot of mole % Or for K-feldspar grains. (b) Plot of wt. % F versus wt. % ΣFeO for muscovite.

Table 3. Representative analysis of sulphide phases from Dunbrack deposit, Nova Scotia.

				Hypogene phases				
Sample	DB-96-3	DB-96-3	DB-96-3	DB-96-1		DB-96-3	DB-96-3	DB-96-1
Point	1	3	4	5		17	18	1
Phase	Cpy	Cpy	Gal	Gal		Sph	Sph	Sph
Weight %								
Cu	34.45	34.93						
Pb			87.44	87.65				
Zn						66.31	66.45	62.95
Fe	30.09	30.66				1.05	0.79	4.80
Ag								
S	34.65	34.77	12.87	12.57		32.63	32.49	32.81
Total	99.19	100.36	100.31	100.23		99.99	99.73	100.56
Atomic %								
Cu	25.08	25.18						
Pb			51.25	51.89				
Zn						49.45	49.72	46.41
Fe	24.92	25.14				0.92	0.69	4.14
Ag								
S	49.99	49.67	48.74	48.10		49.62	49.58	49.33

					Secondary phases					
Sample	DB-96-3	DB-96-3	DB-96-3	DB-96-3	DB-96-1	DB-96-3	DB-96-3	DB-96-3	DB-96-3	DB-96-1	DB-96-1
Point	5	10	14	20	24	8	9	12	22	8	10
Phase	Born	Born	Cov	Cov							
Weight %											
Cu	55.32	53.81	61.16	63.93	68.98	33.44	26.11	16.81	52.39	34.32	43.85
Pb								52.81		31.07	21.24
Zn						21.82	34.78				
Fe	13.15	13.37		3.43		10.11	6.90	12.46	14.36		
Ag										1.63	2.51
S	30.88	31.03	31.02	32.25	29.06	31.12	31.97	22.05	33.30	22.06	25.72
Total	99.35	98.21	92.18	99.61	98.04	96.49	99.76	104.13	100.05	89.08	93.32
Atomic %											
Cu	42.06	41.12	49.38	48.26	54.31	26.15	19.90	18.40	38.88	38.70	42.64
Pb								17.72		10.74	6.30
Zn						16.59	25.76				
Fe	11.38	11.62		2.94		9.00	6.04	15.51	12.13		
Ag										1.08	1.43
S	46.55	47.01	49.64	48.26	45.36	48.24	48.29	47.82	48.98	49.31	49.58

Abbreviations: Cpy, chalcopyrite; Gal, galena; Sph, sphalerite; Born, bornite; Cov, covellite.

Decrepitate analysis

Analysis of decrepitate mounds in areas of clear quartz were performed in order to determine the solute chemistry of the fluid inclusions (e.g., Haynes et al. 1988). The procedure involves decrepitating of fluid inclusions in the heating stage which results in formation of chemical precipitates (e.g., NaCl, $CaCl_2$, KCl) or mounds on the host surface, as illustrated with back-scattered electron images in Figure 13. Analysis of the mounds using a rastering technique with a defocused (10 μm) electron beam indicated that the majority of the mounds formed are equant (Fig. 13a) and consist of NaCl (Fig. 13d). Abundant voids within the quartz (Fig. 13b) may reflect evacuation of low-salinity inclusions. Skeletal mounds (Fig. 13c) are invariably K- and Ca-rich and form a discrete chemical population in Figure 13d. This last group may correspond to those inclusions with low eutectic temperature (i.e., -50°C) in which hydrohalite melted at -35°

to -30°C (i.e., elevated $CaCl_2$ chemistry). Thus, the decrepitate data suggest that two, and possibly three, compositionally distinct fluids may be present.

STABLE ISOTOPES (S, O, D)

Sulphur isotopes

Sulphur isotopic data have been obtained for chalcopyrite (n=1), sphalerite (n=1), and galena (n=3) and $\delta^{34}S$ values range from +6.9‰ (sph) to -3.1‰ (Table 4). The results overlap most of the ^{34}S data for sulphide mineralization in the South Mountain Batholith (Fig. 14). The sphalerite and chalcopyrite represent a sulphide pair from the same sample (DB-96-3), but their $\Delta^{34}S$ value does not yield a reasonable temperature of vein formation (i.e., 250° to 300°C, see below) and suggests disequilibrium. The presence of secondary

b

c

a

Quartz euhedra decorated with
primary and pseudosecondary
inclusions
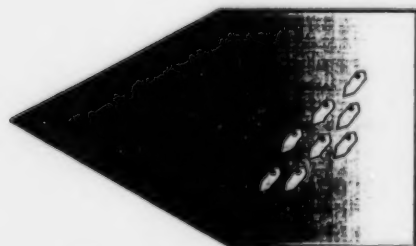
1 Primary Vapor- and liquid-
   rich aqueous inclusions;
   irregular L:V ratios

2 Pseudosecondary inclusions -
   L_{H2O}-V ; uniform L:V ratios

3 Monophase
   aqueous

4 Liquid petroleum

Fig. 10. (a) Schematic illustration of the four types of fluid inclusions hosted by quartz at Dunbrack. (b) Plane of pseudosecondary, negative-shaped, two-phase (L-V) aqueous inclusions in quartz at Dunbrack. These inclusions have very consistent L:V ratios along the healed fracture plane and homogenize at 140 ± 1°C. The largest inclusion is ca. 100 μm wide. (c) Two-phase L-V petroleum inclusions in quartz from Dunbrack. These inclusions are isolated and occur in the same area as inclusions in Figure 10b.
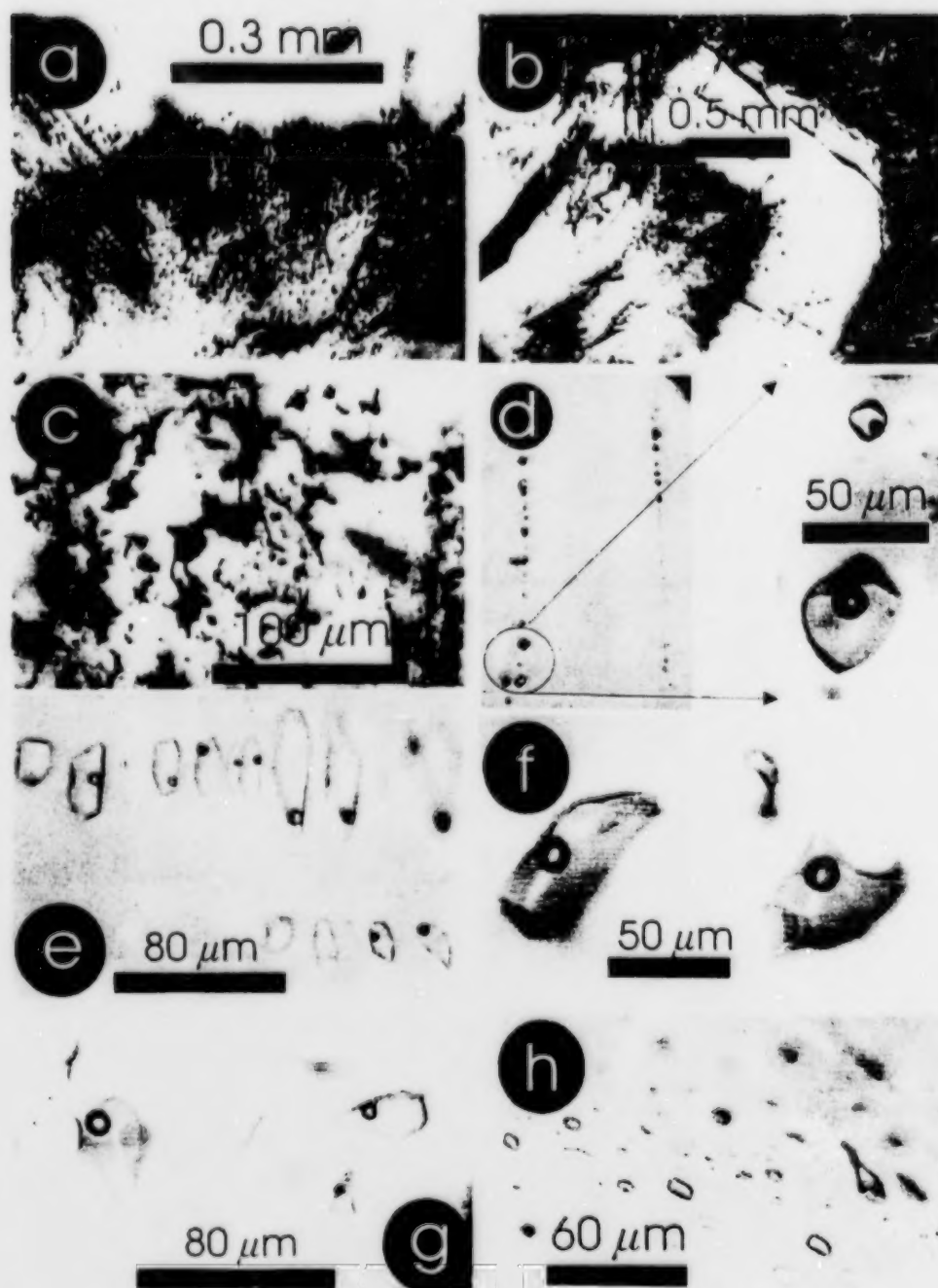
Fig. 11. Photomicrograph of fluid inclusions hosted by vein quartz at Dunbrack. Photos taken in transmitted light. (a, b) Areas inundated with primary fluid inclusions along growth zones in comb quartz. (c) Close-up of area inundated with primary inclusions of irregular shape; in this case the inclusions are dominantly V-rich types and probably reflect post entrapment necking. (d) Two parallel fracture planes decorated by secondary or pseudosecondary, equant- to negative shaped L-V fluid inclusions (enlargement to the right) that homogenize at 140°C. (e) Abundant, elongate to negative-shaped, pseudosecondary, fluid inclusions decorating a healed fracture in comb quartz. These inclusions homogenized at 137 ± 0.5°C (n=20). (f) Isolated L-V fluid inclusions of somewhat irregular shape that occur with equant- and negative-shaped fluid inclusions with similar L:V ratios. (g) Area of irregular-shaped fluid inclusions that show evidence of necking, but note that L:V ratios are consistent which indicates necking occurred prior to separation of the V-phase. (h) Plane of equant-shaped monophase (L) inclusions.
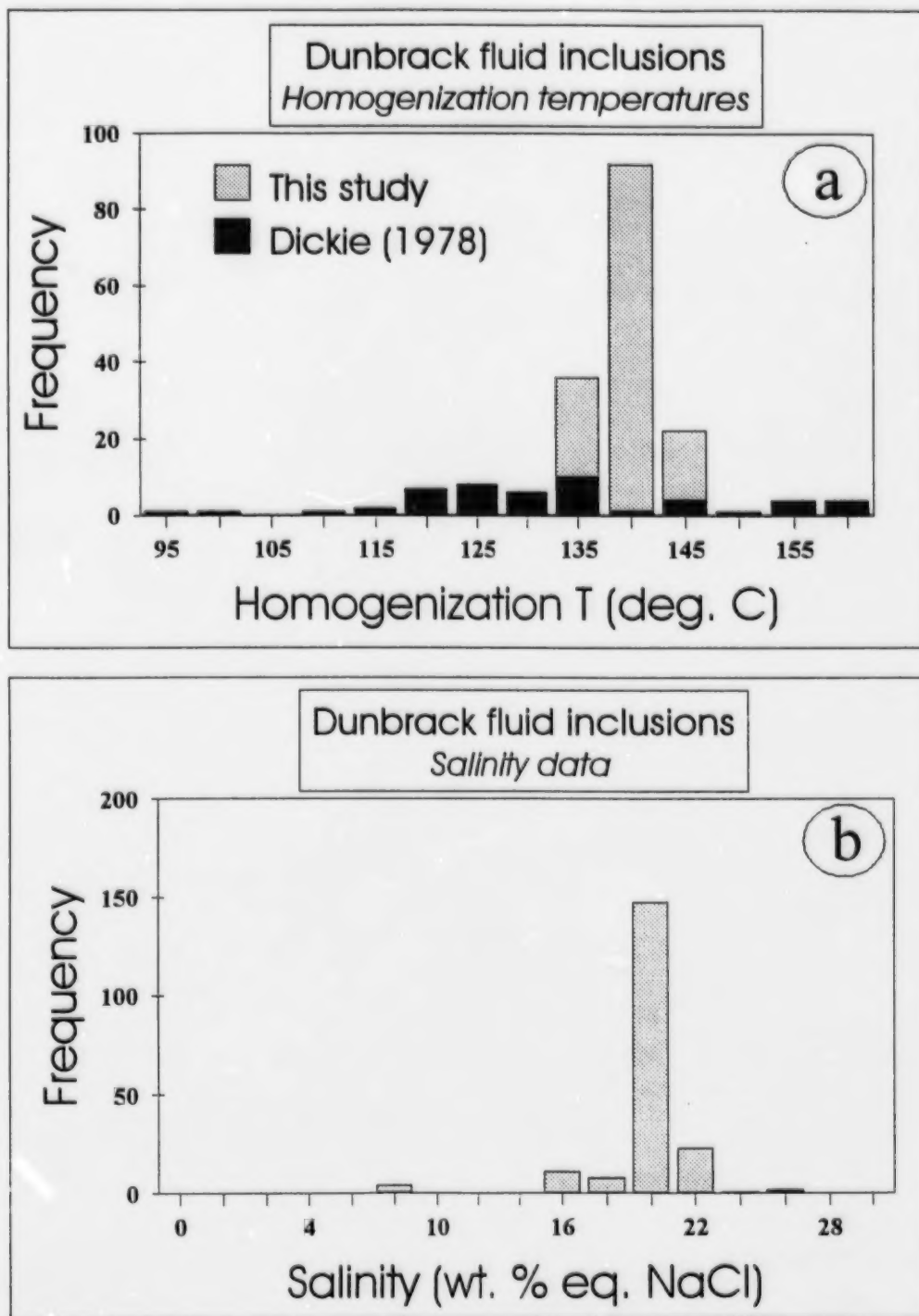
Fig. 12. Histogram plots summarizing homogenization temperatures (a) and salinity measurements (b) on two-phase (L-V) aqueous inclusions in quartz from Dunbrack. Note the difference in homogenization temperatures between this study and those of Dickie (1978), with the latter having a much larger range of values compared to the results of the present study.
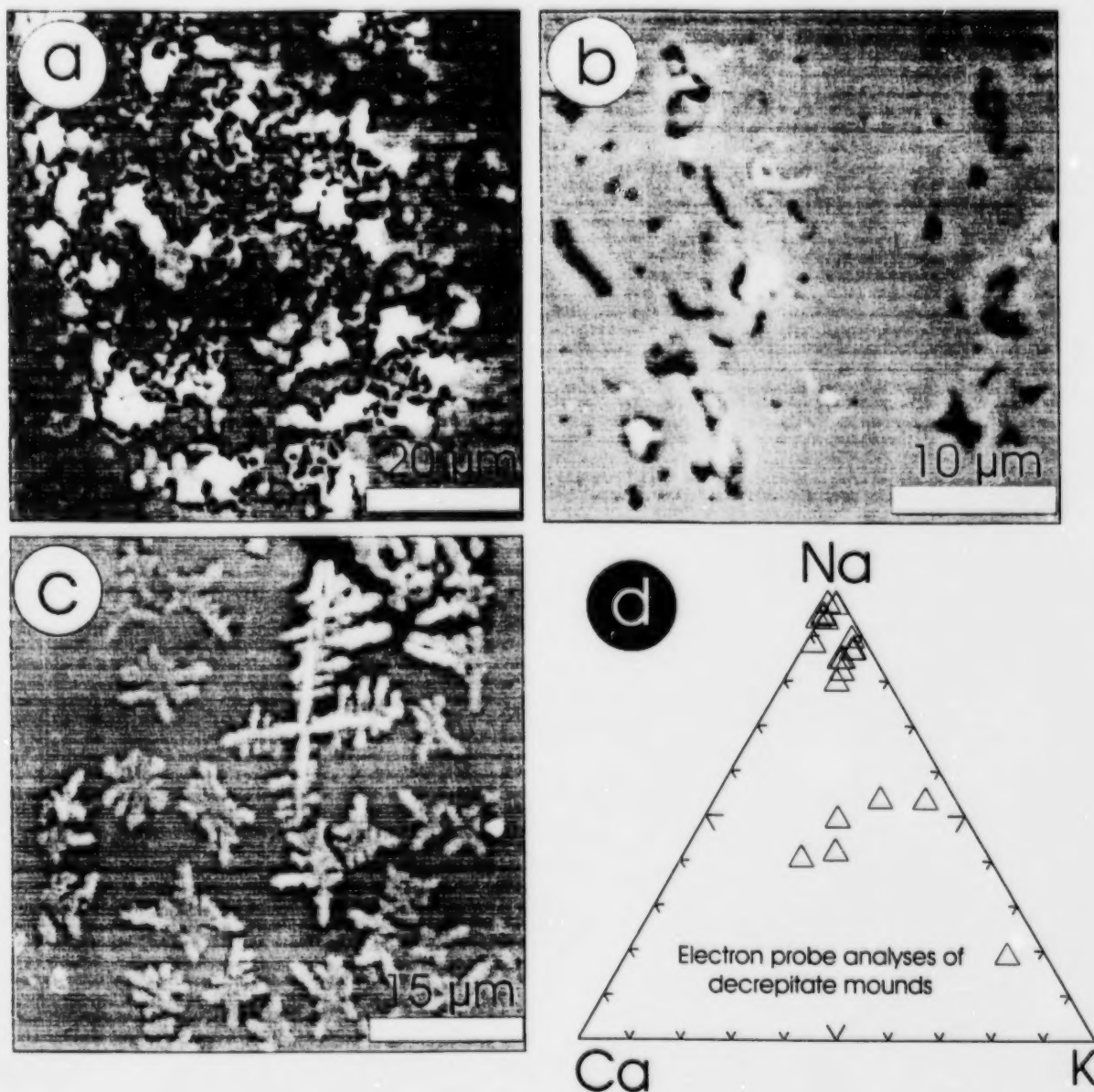
Fig. 13. Back-scattered electron images (a, b, c) and compositional data (d) for decrepitate mounds hosted by quartz from Dunbrack deposit. Note that the dendritic to skeletal shapes in Figure 13c are typical of K-rich salts and correspond to one of the populations in Figure 13d. In contrast, the equant mounds in Figure 13a are Na-rich and plot near the apex of the K-Na-Ca ternary in Figure 13d.

copper sulphides along the margins and internal fractures of chalcopyrite suggest, therefore, that the chalcopyrite δ^{34}S data may not represent a primary signature.

In order to interpret the δ^{34}S data in the context of source reservoirs, fractionation of ^{34}S between mineral and fluid (i.e, Δ^{34}S$_{H_2S\text{-sulphide}}$) must be considered. Using the fractionation factors compiled by Ohmoto and Rye (1979), the δ^{34}S$_{H_2S}$ values of the fluid compute to +4.2 to +6.6‰ for ca. 300°C, except for the anomalous galena sample (DB-96-12) which seems to have been deposited form a fluid with a lighter

δ^{34}S$_{H_2S}$ signature (-1.2‰), possibly reflecting involvement of another reservoir.

Oxygen isotopes

Oxygen isotopes have been determined in nine quartz separates, which represent the variety of textures and colours of quartz present, and in a single sample of kaoiinite. The δ^{18}O data for quartz range from +13.0 to +17.6‰ and average +15.3 ± 1.2‰; there is no distinction of the data that would

Table 4. Summary of isotopic data, Dunbrack deposit.

Sample	Mineral	$\delta^{18}O$ ‰	δD ‰	$\delta^{34}S$ ‰
DB-96-1.1	Qtz	14.3		
DB-96-1.2	Qtz	15.7	-90	
DB-96-3	Qtz	15.5	-91	
DB-96-3	Kaol	17.1	-103	
DB-96-3	Sph			6.9
DB-96-3	Cpy			4.5
DB-96-5.1	Qtz	13	-94	
DB-96-6.2	Qtz	15.2	-100	
DB-96-9	Qtz	14.8	-108	
DB-96-9	Gal			4.2
DB-96-10.1	Qtz	15.9		
DB-96-10.2	Qtz	17.6	-131	
DB-96-10.3	Qtz	15.7	-113	
DB-96-11	Gal			2.3
DB-96-12	Gal			-3.1

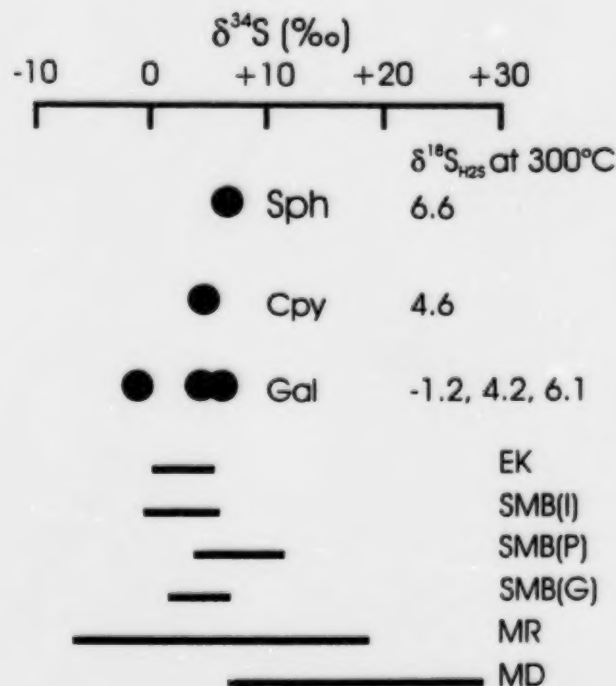Abbreviations: Qtz, quartz; Kaol, kaolinite; Sph, sphalerite; Cpy, chalcopyrite; Gal, galena.

Fig. 14. Sulphur isotope data for sulphides at Dunbrack deposit compared to data for other mineralized sites in the Meguma Terrane. The $\delta^{34}S_{H_2S}$ values calculated with fractionation equations of Ohmoto and Rye (1979). Abbreviations and data sources: EK, East Kemptville (data from Kontak 1990, 1993); SMB(I), South Mountain Batholith - Intrabatholithic; SMB(P), South Mountain Batholith - Peribatholithic (both data sets from A.K. Chatterjee, personal communication 1992); SMB(G), South Mountain Batholith - Granodiorites (data from Poulsen et al. 1991); MR, Meguma Rocks (data from Sangster 1992); MD, Meguma deposits (data from Kontak and Smith 1989, Sangster 1992).

correspond to a particular variety or colour of quartz. However, a variation of up to 2‰ is recorded within one sample from which 3 different generations of quartz were sampled (DB-96-10.1, 10.2, 10.3; Table 4).

Using the quartz-water fractionation equation, the $\delta^{18}O_{water}$ for a given temperature can be determined from the measured $\delta^{18}O_{quartz}$ value (Fig. 15). Assuming a similar temperature of ca. 300°C (see below for reasoning) for precipitation of all quartz samples, the equivalent $\delta^{18}O_{water}$ is +9 to +11.5‰, but a $\delta^{18}O_{water}$ value of +14‰ would characterize the most enriched sample (DB-96-10.2).

The single kaolinite sample analysed for $\delta^{18}O$ has a value of +17.1‰. This value compares, for example, to values of +13.8‰ for late-stage kaolinite at East Kemptville (Kontak 1994), and +17.2 and +18.7‰ for kaolinite from Cornwall, England (Jackson et al. 1982).

Hydrogen isotopes

Fluid inclusions from seven samples of quartz yielded δD values between -90 to -131‰ (avg. -100 ± 14‰) and one kaolinite yielded a value of -103‰. The fluid inclusion δD data have a narrow spread even though they represent sampling of mixed fluid inclusion types. The kaolinite sample has a δD value of -103‰, which overlaps the composition of fluids extracted from quartz.

DISCUSSION

The nature of the vein mineralogy and textures at Dunbrack indicate that hydrothermal fluids exploited an open fracture system, previously used during magma injection to form the dyke. Examination of the vein textures, silicate and sulphide mineralogy, and fluid inclusions permit conclusions to be made regarding the origin of the deposit.

Timing of vein formation

The vein formed after the monzogranite and the footwall dyke, because both have been altered during vein formation. The age of the monzogranite is constrained by the age of the Musquodoboit Batholith, which is ca. 370 Ma as determined by $^{40}Ar/^{39}Ar$ dating of mica (Reynolds et al. 1981; Keppie and Dallmeyer 1987). The new $^{40}Ar/^{39}Ar$ age spectrum on altered felsic dyke rock, despite being of low quality, does provide a minimum age of 366 ± 19 Ma for the hydrothermal activity, given that the sample constitutes part of the vein. Thus, the plateau age is interpreted as representing the timing of hydrothermal activity. The excellent plateau and spot ages of 370 Ma for vein-hosted muscovite are difficult to interpret unequivocally because the muscovite may represent grains
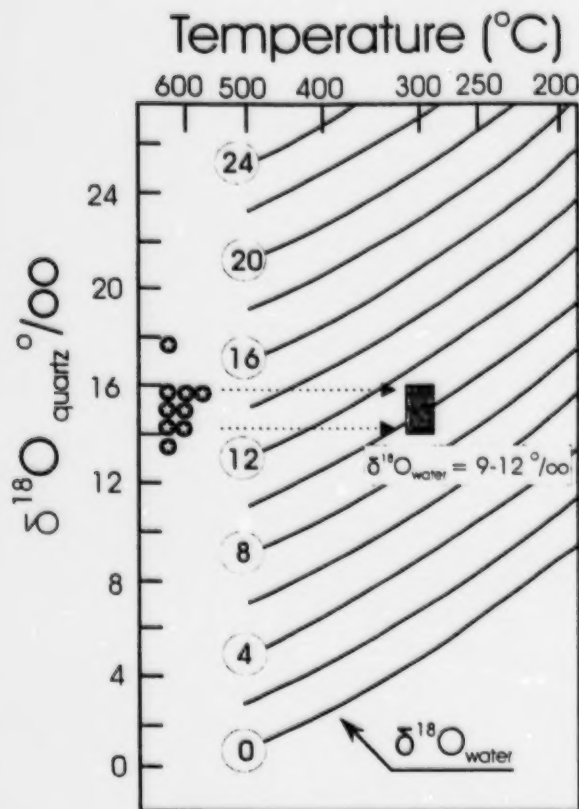
Fig. 15. Plot of $\delta^{18}O$ versus temperature (°C) with isopleths for $\delta^{18}O_{water}$, calculated using quartz-water fractionation equation of Clayton *et al.* (1972); the quartz data shown on left side of diagram. Note that the limiting values of +9 to +11.5‰ for $\delta^{18}O_{water}$, as discussed in the text, are for ca. 300°C.

from wall rock fragments entrained in the vein. Overall the data are consistent with hydrothermal activity at 370 Ma, essentially coeval with the Musquodoboit Batholith.

The 370 Ma age proposed here for dyke emplacement and mineralization contrasts markedly with the ca. 300 Ma age proposed by MacMichael (1975). However, the latter date was obtained on sericitized plagioclase from the wall-rock monzogranite, rather than a pure mineral separate from the vein, as used in this study. MacMichael (1975) noted that the release spectrum is irregular and attributed this to overprinting or possibly weathering. We agree with this conclusion, emphasizing that a later thermal overprint may have been responsible for the sericitic alteration of the plagioclase. For example, sericitized plagioclase in the 373 Ma Port Mouton pluton of southwestern Nova Scotia yielded a much younger Permian $^{40}Ar/^{39}Ar$ age (Fallon 1998).

Nature and Origin of the Vein-Forming Fluid

The composition of the vein minerals, Kf and muscovite, provides some indirect evidence of the nature of the vein-forming fluids. The Kf indicates high temperatures (see

below) and the bulk composition of $Or_{86}Ab_{14}$ suggests a magmatic component to the fluid. The P-rich nature (to 0.4 wt. %) of the Kf suggests affinities to the Musquodoboit Batholith, which is characterized by a P-rich bulk composition (MacDonald and Clarke 1985) and P-enrichment of its Kf (i.e., to 1 wt. % ; unpubl. data of senior author). The composition of the muscovite (i.e., elevated Fe and F) is also consistent with magmatic derivation. The REE pattern of the felsic dyke rock (Fig. 8) is also suggestive of a magmatic origin for the fluid, given that hydrothermal fluids do not transport large amounts of REE (e.g., Wood and Williams-Jones 1994).

The temperature of vein formation can be estimated from the assemblages of vein minerals and fluid inclusion data. The composition of chlorite in two specimens gave a range of temperatures from 80° to 170°C, using known geothermometers [see De Caritat *et al.* (1993) for review], which are in some cases less than the T_h data from fluid inclusions in quartz. The chlorite may have formed after a precursor phase, rather than directly out of the hydrothermal fluid, and so the chlorite data are equivocal. However, these values may indicate that the chlorite formed at this temperature. The composition of Kf can be used qualitatively to infer temperatures using the albite-orthoclase system (e.g., Černý 1994). For the compositions of $Or_{86-100}Ab_{14-0}$, a range of temperatures would be indicated with a maximum at ca. 350°C for the most Ab-rich samples (i.e., $Or_{86}Ab_{14}$). The more Or-rich samples (to Or_{100}) formed at lower temperatures and may, therefore, reflect re-equilibration of originally more sodic compositions during cooling of the system. Based on the stability field of kaolinite, we can infer that it must have formed at less than ca. 300°C because neither diaspore nor pyrophyllite is present in the vein samples (Hemley *et al.* 1980). However, kaolinite is a late overprinting mineral phase at Dunbrack and thus only provides a minimum temperature for the vein.

Estimates of the temperature of vein formation from fluid inclusion homogenization temperatures (T_h) only provide a minimum, because a pressure correction may have to be applied if a homogeneous fluid was trapped. Based on the equant- to negative-crystal shape of the quartz-hosted fluid inclusions, and comparison of the inclusion morphology of Dunbrack samples to those from epithermal environments which formed at 200° to 240°C (e.g., Bodnar *et al.* 1985), higher temperatures must have prevailed and a minimum temperature of ca. 250°C is inferred (T.J. Reynolds, pers. communication, 1996). Based on the aforementioned discussion of whole- rock and mineral chemical data, minimum temperatures of vein formation are estimated at ca. 300° to 350°C. Using this temperature estimate, isochores for fluid salinities of 5 to 25 wt. % eq. NaCl, the dominant fluid composition (see above), indicate a confining pressure of ca. 3 kbars (Fig. 16), which is consistent with pressures inferred during emplacement of the 370 Ma granites of the Meguma Zone (Clarke *et al.* 1997). Because the vein exhibits open-space filling, it is probable that the pressure is some combination of lithostatic and hydrostatic, but the limited vertical extent of the system suggests that a hydrostatic component was minimal.
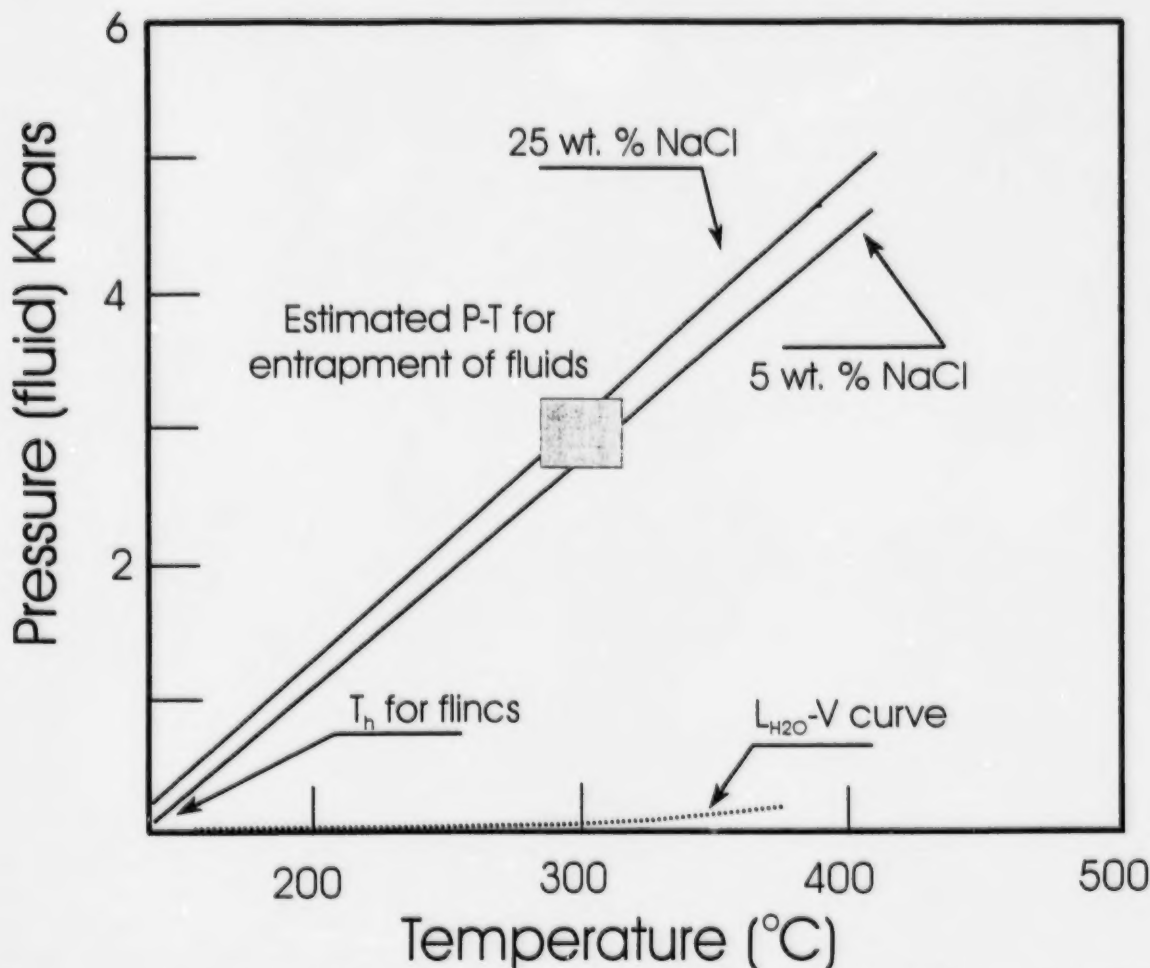
Fig. 16. Pressure-temperature plot showing the projection of isochores for fluid inclusions from Dunbrack and the estimated conditions of entrapment for the fluids based on discussions in the text. The two lines are for 5 and 25 wt. % eq. NaCl aqueous inclusions that homogenized at 140°C; isochores constructed using the program FLINCOR (Brown 1989). The isochores represent the $NaCl-H_2O$ type fluids which form the most abundant fluid inclusion population at Dunbrack.

Fluid inclusion data indicate at least two moderately saline (ca. 20 wt. % eq. NaCl) fluids are present, a $NaCl-H_2O$ fluid and a $NaCl-CaCl_2-KCl-H_2O$ fluid, but the former is clearly the dominant fluid type based on the abundance of inclusions. These compositions are consistent with a magmatic reservoir (Roedder 1984), although the Ca-rich nature of the second fluid is also consistent with interaction of a fluid with or infiltration of a fluid from metamorphic rocks, as represented by the Meguma Group (e.g., Wilkinson 1990; Evans 1995; Pasteris *et al.* 1995). In addition, there is no indication from the inclusions that a meteoric fluid was involved in vein formation.

The sulphur isotope data are uniform in terms of the calculated $\delta^{34}S_{H_2S}$ at +4.2 to +6.6‰, except for the single anomalous galena sample which gave a value of -1.2‰. The former values correspond to magmatic sulphur (Ohmoto and Rye 1979) and indicate, therefore, that sulphur was derived either directly from a magma or via dissolution of magmatic sulphides. These values are similar to the $\delta^{34}S_{H_2S}$ for sulphides

at the East Kemptville tin-base metal deposit (Kontak 1990, 1993) and intrabatholithic sulphide mineralization in the South Mountain Batholith, as compiled in Figure 14. The anomalous $\delta^{34}S_{H_2S}$ value for one galena sample, despite being similar to the other two galena samples, might relate to weathering, disequilibrium processes, or indicate another reservoir for sulphur. The latter scenario is supported by the range of sulphur isotope data for the Meguma Group (Fig. 14) and, as discussed below, additional data that suggest possible incursion of an external fluid which equilibrated with the Meguma Group.

The nature of the fluid(s) responsible for vein formation is evaluated in terms of $\delta D-\delta^{18}O$ signature in Figure 17. Whereas the $\delta^{18}O$ values overlap the field for magmatic and/or metamorphic fluids, the δD values are clearly displaced from these fields, suggesting that another process or processes was/were involved. Firstly, the trend of the data in Figure 17 does not define a mixing line, suggesting that fluid compositions do not represent simple mixing of two fluids, but
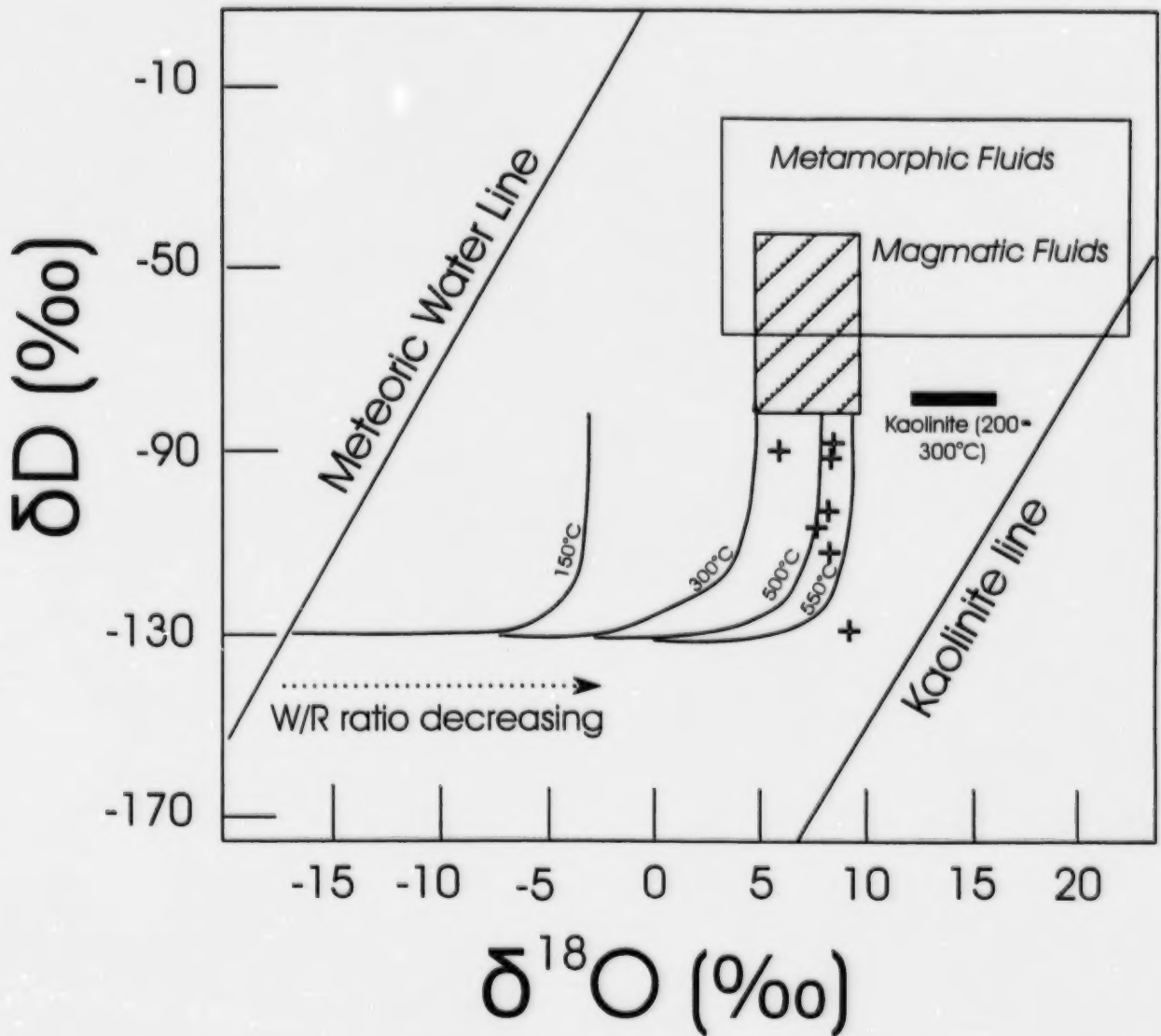
Fig. 17. Plot of δD versus δ¹⁸O for vein forming fluids at Dunbrack, as represented by the crosses, compared to fields for magmatic and metamorphic waters, the meteoric water line and the kaolinite line. The points calculated for 300°C using quartz-water fractionation factor of Clayton *et al.* (1972). The curved lines show the evolution of a fluid of meteoric origin with δD of -130‰ that interacts with granite at different temperatures, as indicated on the curves (modified from Taylor 1987) The thick kaolinite line shows the range for fluid in equilibrium with the kaolinite analyzed at Dunbrack for limiting temperatures of 200-300°C, using the fractionation equations of Suzuoki and Epstein (1976) and Kulla and Anderson (1978) for D and ¹⁸O, respectively.

instead water-rock interactions (Sheppard 1986). Although the low δD values suggest a possible model of interaction of meteoric waters at varying water:rock ratios (e.g., Sheldon *et al.* 1986) and elevated temperatures (W/R in Fig. 17), neither the fluid inclusion data (see above) nor the required paleolatitude of the Meguma Zone at ca. 370 Ma (Keppie 1977) support involvement of such a low-D (i.e., -130‰) meteoric water. Magmatic degassing can also generate low-D waters, but this model is not considered realistic given that it is usually documented in large, shallow-level magmatic-hydrothermal systems (e.g., Taylor 1988). Instead, the low δD

values for the Dunbrack fluids are interpreted to reflect interaction of a fluid with organic (graphitic) material to produce organic water, the interaction of which is known to reduce the δD value of a fluid (see discussion of Sheppard 1986). Based on this interpretation, the δD data indicate interaction of a primary magmatic fluid with the country rock of the Meguma Group or alternatively, incursion of a metamorphically generated fluid, perhaps formed during contact metamorphism accompanying intrusion of the Musquodoboit Batholith. Regardless of the interpretation, more than one reservoir is required to account for the δD-δ¹⁸O

data. A similar interpretation of low δD fluids has been made for granite-hosted Sn-W mineralization in Thailand (Linnen and Williams-Jones 1994; Linnen 1998).

The kaolinite data shown in Figure 17 plot away from the quartz data, but are proximal to the magmatic field. However, most importantly the ^{18}O-D data for kaolinite fall well away from the line defining kaolinite formed from weathering. Thus, the Dunbrack kaolinite is inferred to be of hypogene origin and probably formed during the waning stages of the hydrothermal system.

SUMMARY

Mineralogical, geochemical, stable isotopic, fluid inclusion, and geochronological data for a mineralized vein at the Dunbrack Pb-Zn-Cu-Ag deposit indicate that the mineralization occurred at ca. 370 Ma from dominantly magmatic fluids. However, both the compositions of fluid inclusions, as determined from thermometry and analysis of decrepitate mounds, and isotopic data indicate that whereas the magmatic fluid was responsible for mineralization, minor involvement of an externally-derived fluid probably occurred. The proximity of a fine-grained leucomonzogranite body at the west end of the vein (i.e., near Pace Lake in Figure 2) and the presence of a fine-grained dyke rock adjacent to the mineralized vein are both reasons to infer a local source with generation of a late-stage fluid from an evolved, volatile-rich, felsic magma. That the vein is strongly controlled by structure indicates that the fluid exploited a pre-existing weakness. The exceptional quartz textures (e.g., cockade, comb; Figs. 3, 4) at Dunbrack are commonly associated with epithermal-type settings (e.g., Shimizu *et al.* 1998). However, Dowling and Morrison (1988) noted that such textures also occur in the plutonic environment at levels beneath the epithermal setting. In the case of Dunbrack, the nature of the mineralized quartz vein is suggestive of a fault-jog style vein (Hodgson 1989) which would generate a cavity for open space textures to develop, as originally proposed by MacMichael (1975) and reiterated here.

ACKNOWLEDGEMENTS

BODNAR. R.J., REYNOLDS, T.J. and KUEHN, C.A. 1985. Fluid inclusion systematics in epithermal systems. In Geochemistry of Epithermal Systems, *Edited by* B.R. Berger and P.M. Bethke. Reviews in Economic Geology, 2, pp. 73-97.

BROWN, P.E. 1989. FLINCOR: A microcomputer program for the reduction and investigation of fluid inclusion data. American Mineralogist, 74, pp. 1390-1393.

ČERNÝ, P. 1994. Evolution of feldspars in granitic pegmatites. In Feldspars and Their Reactions, *Edited by* I. Parsons. Kluwer Academic Publishers, The Netherlands, pp. 501-540.

CHATTERJEE,. A.K. 1977. Comments on the Association of tridymite, pyromorphite and meneghinite from Dunbrack prospect. Nova Scotia Department of Mines and Mineral Resources Division, Report of Activities, pp. 95-102.

CLARKE, D.B., MACDONALD, M.A., and TATE, M.C. 1997. Late Devonian mafic-felsic magmatism in the Meguma Zone, Nova Scotia. Geological Society of America, Memoir 191, pp. 107-127.

CLAYTON, R.N., O'NEIL, J.R., and MAYEDA, T.K. 1972. Oxygen isotope exchange between quartz and water. Journal of Geophysical Research, 77, pp. 3057-3067.

COREY, M.C. 1993. Polymetallic W-Mo mineralization and associated alteration in the eastern Musquodoboit Batholith. In Mines and Minerals Branch, Report of Activities 1992, Nova Scotia Department of Natural Resources, Mines and Energy Branches Report 93-1, pp. 31-44.

––––– 1995. Diamond-drilling in the Tobeatic Shear Zone of southwestern Nova Scotia and the potential for epithermal-style bas and precious metals. In Mines id Minerals Branch, Report of Activities 1994, Nova Scotia Department of Natural Resources, Mines and energy Branches Report 95-1, pp. 27-42.

––––– and Graves, R.M.1996. Investigation of epithermal-type, breccia-hosted Pb-Zn-Ba-Au mineralization within the Tobeatic Shear Zone of southwestern Nova Scotia. Nova Scotia Department of Natural Resources, Minerals and Energy Branch, Open File Report 96-008.

CRAWFORD, M.L. 1981. Phase equilibria in aqueous fluid inclusions. In Fluid Inclusions: Applications to Petrology, *Edited by* L.S. Hollister and M.L. Crawford. Mineralogical Association Canada Short Course Handbook 6, pp. 75-100.

DE CARITAT. P., HUTCHEON, I. and WALSHE, J.L., 1993. Chlorite geothermometry: a review. Clays and Minerals, 41, pp. 219-239.

DICKIE, J.R. 1978. Geological, mineralogical and fluid inclusion studies at the Dunbrack lead-silver deposit, Musquodoboit Harbour, Halifax County, Nova Scotia. Unpublished B.Sc. thesis, Dalhousie University, Halifax.

DONG, G.Y. and MORRISON, G.W. 1995: Adularia in epithermal veins, Queensland: morphology, structural state and origin. Mineralium Deposita, 30, pp. 11-19.

DONG, G.Y., MORRISON, G.W. and JAIRETH, S. 1995. Quartz textures in epithermal veins, Queensland - classification, origin and implication. Economic Geology, 90, pp.1841-1856.

DONG, G.Y. and ZHOU, T. 1996. Zoning in the Carboniferous-Lower Permian Cracow epithermal vein system, central Queensland, Australia. Mineralium Deposita, 31, pp.210-224.

DOWLING, K. and MORRISON, G. 1988. Application of quartz textures to the classification of gold deposits using North Queensland examples. Economic Geology, Monograph 6, pp. 342-355.

ERDMER, P., GHENT, E.D., ARCHIBALD, D.A. and STOUT, M.Z. 1998. Paleozoic and Mesozoic high-pressure metamorphism at the margin of ancestral North America in central Yukon. Geological Society America Bulletin, 110, pp. 615-629.

EVANS, M.A. 1995. Fluid inclusions in veins from the Middle Devonian shales: A record of deformation conditions and fluid evolution in the Appalachian Plateau. Geological Society of America Bulletin, 107, pp. 327-339.

FALLON, R.P. 1998. Age and thermal history of the Port Mouton Pluton, southwest Nova Scotia: A combined U-Pb, ^{40}Ar/^{39}Ar age spectrum, and ^{40}Ar/^{39}Ar laserprobe study. Unpublished M.Sc. Thesis, Dalhousie University, Halifax, Nova Scotia.

FORD, K.L. 1993. Radioelement mapping of parts of the Musquodoboit Batholith and Liscomb Complex, Meguma Zone, Nova Scotia. In Mineral Depoist Studies in Nova Scotia, 2,

Edited by A.L. Sangster. Geological Survey of Canada, Paper 91-9, pp. 71-111.

FRIEDLAENDER, C.G.I. 1968. Tridymite in mineralized zone at Dunbrack, Musquodoboit River, Nova Scotia. The Canadian Mineralogist, 9, pp. 572.

_____ 1970. Tridymite in the gangue of a Pb-Cu-Zn occurrence. Schweiz. Min. Petrol. Mitt., 50, pp. 183-199.

HAM, L. 1993. A progress report on the Musquodoboit Batholith project. *In* Mines and Minerals Branch, Report of Activities 1992, Nova Scotia Department of Natural Resources, Mines and Minerals Branches Report 93-1, pp. 45-59.

_____ 1994. An update on the Musquodoboit Batholith project. *In* Mines and Minerals Branch, Report of Activities 1992, Nova Scotia Department of Natural Resources, Mines and Minerals Branches Report 93-1, pp. 131-136.

_____ 1998. Musquodoboit Batholith project and the geology of the Tangier Grand Lake area. *In* Mines and Minerals Branch, Report of Activities 1992, Nova Scotia Department of Natural Resources, Mines and Minerals Branches Report 93-1, pp. 3-10.

HAYNES, F.M., STERNER, S.M. and BODNAR, R.J. 1988. Synthetic fluid inclusions in natural quartz. IV Chemical analyses of fluid inclusions by SEM/EDA: Evaluation of the method. Geochimica Cosmochimica Acta, 52, pp. 959-977.

HEMLEY, J.J., MONTOYA, J.W., MARIENKO, J.W. and LUCE, R.W. 1980. Equilibrium in the system Al_2O_3-SiO_2-H_2O and some general implications for alteration/mineralization processes. Economic Geology, 75, pp.210-228.

HODGSON, C.J. 1989. The structure of shear-related, vein-type gold deposits: A review. Ore Geology Reviews, 4, pp. 231-273.

HORNE, R. J., COREY, M.C., HAM, L.J. and MAC DONALD, M.A. 1992. Structure and emplacement of the South Mountain Batholith, southwestern Nova Scotia. Atlantic Geology, 28, pp. 29-50.

HORNE, R.J., MACDONALD, L., BHATNAGAR, P., and TÉNIÈRE, P. 1998. Preliminary bedrock geology of the Lucasville-Lake Major area, central Meguma mapping project, central Nova Scotia. *In* Nova Scotia Department of Natural Resources, Report of Activities. *Edited by* D.R. MacDonald and K.A. Mills. Report 98-1, pp. 15-26.

JACKSON, N.J., HALLIDAY, A.N., SHEPPARD, S.M.F. and MITCHELL, J.G. 1982. Hydrothermal activity in the St. Just Mining District, Cornwall, England. *In* Metallization Associated with Acid Magmatism, *Edited by* A.M. Evans, John Wiley & Sons Ltd., pp. 137-179.

JENNER, G.A., LONGERICH, H.P., JACKSON, S.E., and FRYER, B.J.1990. ICP-MS - a powerful tool for high precision trace element analyses in earth sciences: evidence from analysis of selected USGS reference samples. Chemical Geology, 83, pp. 133-148.

JONES, J.B. and MACMICHAEL, T.P. 1976. Observations of the geology of a portion of the Musquodoboit Harbour batholith. Nova Scotia Department of Mines, Mineral Resources Division, Report of Activities, Report 76-2, pp. 63-71.

KEPPIE, J.D., 1977. Plate tectonic interpretation of Paleozoic world maps (with emphasis on circum-Atlantic orogens and southern Nova Scotia). Nova Scotia Department of Mines, Paper 77-3.

_____ and DALLMEYER, R.D. 1987. Dating transcurrent terrane accretion: an example from the Meguma and Avalon composite terranes in the northern Appalachians. Tectonics, 6, pp. 831-847.

KONTAK, D.J. 1990. A sulfur isotope study of main-stage tin and base metal mineralization at the East Kemptville tin deposit, Yarmouth County, Nova Scotia: evidence for magmatic origin of metals and sulphur. Economic Geology, 85, 399-407.

_____ 1993 Sulphur enrichment in late stage veins, East Kemptville tin and base metal deposit, Nova Scotia, Canada: evidence for late incursion of metasedimentary-processed sulfur in a magmatic system. Economic Geology, 88, pp. 201-205.

_____ 1994. Geological, geochemical and isotopic studies of the East Kemtpville Sn-(Zn-Cu-Ag) deposit, Yarmouth County, Nova Scotia, Canada. Proceedings of the Eighth Quadrennial IAGOD Symposium, E. Schweizerbart'sche Verlagsbuch-handlung, pp.383-409.

_____ 1998. A study of fluid inclusions in sulphide and nonsulphide mineral phases from a carbonate-hosted Zn-Pb deposit, Gays River, Nova Scotia. Economic Geology, 93, pp. 793-817.

KONTAK, D.J. and SMITH, P.K. 1993. A metaturbidite-hosted lode gold deposit: The Beaver Dam deposit, Nova Scotia. I. Vein paragenesis and mineral chemistry. Canadian Mineralogist, 31, pp. 471-522.

KONTAK, D.J., HORNE, R.J. and SMITH, P.K. 1996. Hydrothermal characterization of the West Gore Sb-Au deposit, Meguma Terrane, Nova Scotia, Canada. Economic Geology, 91, pp. 1239-1262.

KONTAK, D.J., HORNE, R.J., ANSDELL, K. and ARCHIBALD, D.A. under review. Carboniferous Barite-Fluorite Mineralization in the 370 Ma Kinsac Pluton, southern Nova Scotia. Atlantic Geology.

KULLA, J.B. and ANDERSON, T.F. 1978. Experimental oxygen isotope fractionation between kaolinite and water. Short Papers of the 4th International Conference on Geochronology, Cosmo-chronology and Isotope Geology, 1978, U.S. Geological Survey, Open File Report 78-701.

LINNEN, R.L. 1998. Depth of emplacement, fluid provenance and metallogeny in granitic terranes: a comparison of western Thailand with other tin belts. Mineralium Deposita, 33, pp. 461-476.

_____ and WILLIAMS-JONES, A.E. 1994. The evolution of pegmatite-hosted tin mineralization at Nong Sua, Thailand: evidence from fluid inclusions and stable isotopes. Geochimica et Cosmochimica Acta, 58, pp. 735-747.

MACDONALD, M.A. and CLARKE, D.B. 1985. The petrology, geochemistry and economic potential of the Musquodoboit Batholith, Nova Scotia. Canadian Journal of Earth Sciences, 22, pp. 1633-1642.

MACMICHAEL, T.P. 1975. The origin of the lead-zinc-silver ores and alteration of the surrounding granite at the Dunbrack mine, Musquodoboit Harbour, Nova Scotia. Unpublished B.Sc. thesis, Dalhousie University, Halifax.

OHMOTO, H. and RYE, R.O. 1979. Isotopes of sulphur and carbon. *In* Geochemistry of Hydrothermal Ore Deposits. *Edited by* H.L. Barnes. Wiley Interscience, New York, pp. 50-567.

PASTERIS, J.D., HARRIS, T.N. and SASSANI, D.C. 1995. Interactions of mixed volatile-brine fluids in rocks of the southwestern footwall of the Duluth Complex, Minnesota: Evidence from aqueous fluid inclusions. American Journal of Science, 295, pp. 125-172.

REYNOLDS, P.H., ZENTILLI, M. and MUECKE, G.K. 1981: K-Ar and $^{40}Ar/^{39}Ar$ geochronology of granitoid rocks from southern Nova Scotia: its bearing on the geological evolution of the Meguma zone of the Appalachians. Canadian Journal of Earth Sciences, 18, pp. 386-394.

ROEDDER, E. 1984. Fluid Inclusions. Mineralogical Society of America. Reviews in Mineralogy, 12, 644 p.

SANDER, M.V. and BLACK, J.E. 1988. Crystallization and recrystallization of growth-zoned vein quartz crystals from epithermal systems- implications for fluid inclusion studies. Economic Geology, 83, pp. 1052-1060.

SANGSTER, A.L. 1992. Light stable isotope evidence for a metamorphic origin for bedding parallel, gold bearing veins in Cambrain flysch. Meguma Group, Nova Scotia. Exploration Mining Geology, 1, pp. 69-79.

SHELTON, K.L., TAYLOR, R.P., and SO, C.S. 1986. Stable isotope studies of the Dae Hwa tungsten-molybdenum mine, Republic of Korea: evidence of progressive meteoric water interaction in a tungsten-bearing hydrothermal system. Economic Geology,

82, pp. 471-481.

SHEPPARD, S.M.F. 1986. Characterization and isotopic variations in natural waters. *In* Stable Isotopes in High Temperature Geological Processes, *Edited by* J.W. Valley, H.P. Taylor, Jr., and H.R. O'Neil. Mineralogical Society of America Reviews in Mineralogy, 16, pp. 165-184.

SHIMIZU, T., MATSUEDA, H., ISHIYAMA, D. and MATSUBAYA, O. 1998. Genesis of epithermal Au-Ag mineralization of the Koryu Mine, Hokkaido, Japan. Economic Geology, 93, 303-325.

STANTON, R.L. 1972. Ore Petrology. McGraw-Hill Book Company, Toronto, 713 p.

SUZUOKI, T. and EPSTEIN, S. 1976. Hydrogen isotope fractionation between OH-bearing minerals and water. Geochimica et Cosmochimica Acta, 40, pp. 1229-1240.

TAYLOR, B.E. 1987. Stable isotope geochemistry of ore-forming systems. *In* Short Course in Stable Isotope Geochemistry of Low Temperature Fluids, *Edited by* T.K. Kyser. Mineralogical Association of Canada, 13, pp. 337-418.

———— 1988. Degassing of rhyolitic magmas: hydrogen isotope evidence and implications for magmatic-hydrothermal ore deposits. In Recent Advances in the Geology of Granite-Related Mineral Deposits, *Edited by* R.P. Taylor and D.F. Strong. Canadian Institute Mining and Metallurgy, Special Volume 39, pp. 33-49.

VEARNCOMBE, J.R. 1993. Quartz vein morphology and implications for formation depth and classification of Archaean gold-vein deposits. Ore Geology Reviews, 8, pp. 407-424.

WILKINSON, J.J. 1990. The role of metamorphic fluids in the development of the Cornubian orefield: fluid inclusion evidence from south Cornwall. Mineralogical Magazine, 54, pp. 2219-230.

WOOD, S. and WILLIAMS-JONES, A.E. 1994. The aqueous geochemistry of the rare-earth elements and yttrium. 4. Monazite solubililty and REE mobility in exhalative massive sulphide-depositing environments. Chemical Geology, 115, pp. 47-60.